

Stabilizer ground states: theory, algorithms and applications

Jiace Sun,¹ Lixue Cheng,^{1,2} and Shi-Xin Zhang³

¹*Division of Chemistry and Chemical Engineering,
California Institute of Technology, Pasadena, CA 91125, USA*^{*}
²*Microsoft Research AI4Science Lab, Berlin 10178, Germany*
³*Tencent Quantum Laboratory, Shenzhen 518057, China*

Stabilizer states have been commonly utilized in quantum information, quantum error correction, and quantum circuit simulation due to their simple mathematical structure. In this work, we apply stabilizer states to tackle quantum many-body problems and introduce the concept of stabilizer ground states. We present a simplified equivalent formalism for identifying stabilizer ground states of general Pauli Hamiltonians. Moreover, we also develop an exact and linear-scaled algorithm to obtain stabilizer ground states of 1D local Hamiltonians and thus free from discrete optimization. This proposed theoretical formalism and linear-scaled algorithm are not only applicable to finite-size systems, but also adaptable to infinite periodic systems. The scalability and efficiency of the algorithms are numerically benchmarked on different Hamiltonians. Finally, we demonstrate that stabilizer ground states can find various promising applications including better design on variational quantum algorithms, qualitative understanding of phase transitions, and cornerstones for more advanced ground state ansatzes.

I. INTRODUCTION

Discovering the ground state of quantum Hamiltonians represents one of the significant quests in the domain of quantum many-body physics. However, the reality stands that exact computations of ground states are impractical in most cases, due to the exponential growth of the Hilbert space dimension [1–6]. Therefore, it is important to leverage simple and scalable data structures to approximate ground states efficiently, either for qualitative analysis of the low-energy physics of the Hamiltonian or for further developments of advanced methods on top of these approximated ground states.

The typical forms of wavefunction approximation ansatz $|\psi\rangle$ and methods include ground states of free Hamiltonians (mean-field approaches), tensor network states (density matrix renormalization group) [7–9] and neural network states (variational quantum Monte Carlo approach) [10–15]. According to the Rayleigh-Ritz principle [16], these approximations can be derived via a unified variational optimization framework formulated as $|\psi\rangle = \operatorname{argmin}_{|\psi\rangle} \langle\psi|H|\psi\rangle$. These approximated ground states can further serve as the cornerstones in developing advanced numerical methods. For instance, in the realm of quantum chemistry, several accurate theories, such as Møller–Plesset perturbation theory [17] and coupled cluster theory [18, 19], have been established based on the Hartree–Fock state [20, 21] derived from mean-field approximations. This underscores the important role of these approximations in facilitating the development of advanced theories in quantum many-body problems.

The ideas of Clifford operations and stabilizer states have been developed during the advancements of quantum computing [22, 23]. Clifford operations are a set of quantum operations generated from CNOT, Hadamard, and phase gates, and stabilizer states are the quantum states generated exclusively by applying Clifford operations. Stabilizer states can be tracked by the corresponding Pauli stabilizers, which give a polynomial-sized classical description [24, 25]. Although stabilizer states are defined on the qubit space, they can also be applied to fermionic Hamiltonian via Jordan-Wigner [26] or Brayvi-Kitaev transformation [27] and bosonic Hamiltonians via proper truncation and encodings [28–31]. Stabilizer states are able to not only capture long-range area-law entanglement that is significant for understanding topological order and symmetry-protected topological states [32]; but also characterize volume-law entanglement [33], which is a feature not typically achievable by other ansatzes, such as the widely recognized matrix product states [34]. Thanks to these features, Clifford operations and stabilizer states are utilized as important tools in the explorations of quantum information [35, 36], quantum dynamics [37–39], quantum error correction [40, 41], topological quantum computing [42], quantum circuit simulation [43–45], and quantum-classical hybrid algorithms [46–50].

In this work, we apply stabilizer states to quantum many-body problems and introduce the concept of the stabilizer ground state which is defined as the stabilizer state with the minimum energy expectation with respect to

^{*} jsun3@caltech.edu.

the Hamiltonian. Due to $O(2^{\frac{1}{2}(n+1)(n+2)})$ number of n -qubit stabilizer states [51], brute-force searching the exact stabilizer ground state is computationally infeasible. Therefore, we introduce the formalism of the restricted maximally-commuting Pauli subset of the Hamiltonian and prove its equivalence to the stabilizer ground state. As a significant contribution, we further present an exact and linear-scaled algorithm to find the stabilizer ground states of 1D local Hamiltonians. For properly defined sparse Hamiltonians, this exact 1D local algorithm is proved to be computationally efficient with a scaling of $O(n \exp(Ck \log k))$ with some constant C , where n is the number of qubits and k represents the locality. Both the formalism for general Hamiltonians and the linear-scaled algorithm for 1D local Hamiltonians can be also extended to infinite periodic systems. Stabilizer ground states and the corresponding exact 1D local algorithms have broad applicability and profound generality for diverse problems, including understanding phase transitions and generating better initial states for variational quantum eigensolver (VQE) problems. We additionally reveal how stabilizer ground states can serve as cornerstones in the development of advanced ground state ansatzes to provide more accurate quantum state descriptions. We envision stabilizer ground states as a pivotal foundation for a wide range of interesting applications, and highlight the collective power of the theories, algorithms, and applications for stabilizer ground states to advance the field of quantum physics.

This paper is organized as follows. We first introduce the notations and mathematical backgrounds of stabilizer states in Sec II A. The equivalence between the stabilizer ground state and the restricted maximally-commuting Pauli subset for general Hamiltonians is derived in Sec. II B, and the exact linear-scaled algorithm for stabilizer ground states of 1D local Hamiltonians is further presented in Sec. II C. Sec. II D extends both the theoretical formalism for general Hamiltonians and the algorithm for 1D local Hamiltonians to infinite periodic systems. Sec. III A and III B benchmark the exact 1D local algorithm on example Hamiltonians by numerically verifying the computational scaling and comparing the performances with numerically optimized stabilizer ground states, respectively. In Sec. III C and III D, we showcase the applications of stabilizer ground states and the corresponding algorithms for generating initial states for VQE problems and qualitative analysis of topological phases. As an illustration of developing advanced ground state wavefunction ansatz, we introduce the extended stabilizer ground state and demonstrate its expressive power on a generalized 2D toric code model in Sec. III E. Finally, we draw conclusions and outline future directions for the development and applications of stabilizer ground states in Sec. IV.

II. THEORY

A. Notations and mathematical background of stabilizer groups

We first revisit the definitions and a few frequently used properties of Pauli operators and stabilizer groups [22, 40].

Let $\mathcal{P}_n = \pm\{I, X, Y, Z\}^{\otimes n}$ represent the set of Hermitian n -qubit Pauli operators. It is important to clarify that \mathcal{P}_n itself is not a group since \mathcal{P}_n does not include anti-Hermitian operators. For any two elements $P_i, P_j \in \mathcal{P}_n$, P_i and P_j either commute or anticommute. A Pauli operator Q commutes with a set of Pauli operators $\mathbf{P} = \{P_i\}$, denoted as $[Q, \mathbf{P}] = 0$, if $[Q, P] = 0$ for each $P \in \mathbf{P}$. We denote it as $[Q, \mathbf{P}] \neq 0$ if Q anticommutes with any $P \in \mathbf{P}$.

A stabilizer group \mathbf{S} is a subset of \mathcal{P}_n that forms a group and satisfies $-I \notin \mathbf{S}$. Any two elements P, Q in \mathbf{S} commute with each other, otherwise $PQPQ = -I$ violates the definition. $\langle \mathbf{P} \rangle = \langle P_1, \dots, P_l \rangle = \{\prod_{Q \in \mathbf{Q}} Q \mid \mathbf{Q} \subseteq \mathbf{P}\}$ is the stabilizer group generated by a set of Pauli operators $\mathbf{P} = \{P_{i=1}^l\}$, if $\langle \mathbf{P} \rangle$ satisfies the definition of stabilizer group. We say \mathbf{P} is a set of generators of the stabilizer group \mathbf{S} when $\mathbf{S} = \langle \mathbf{P} \rangle$. An n -qubit stabilizer group \mathbf{S} has at most n independent generators $\mathbf{g} = \{g_i\}$ and 2^n elements. If $|\mathbf{g}| = n$, \mathbf{S} is a full stabilizer group and we have either $P \in \mathbf{S}$ or $-P \in \mathbf{S}$ (denoted as $P \in \pm \mathbf{S}$) for any $[P, \mathbf{S}] = 0$, $P \in \mathcal{P}_n$.

We say state $|\psi\rangle$ is stabilized by $P \in \mathcal{P}_n$ if $P|\psi\rangle = |\psi\rangle$. We define the stabilizer group of a given $|\psi\rangle$ as $\text{Stab}(|\psi\rangle) = \{P \mid P|\psi\rangle = |\psi\rangle\}$, and $|\psi\rangle$ is a stabilizer state when $\text{Stab}(|\psi\rangle)$ is a full stabilizer group. The mapping $|\psi\rangle \rightarrow \text{Stab}(|\psi\rangle)$ from stabilizer states to full stabilizer groups is a one-to-one correspondence.

B. Stabilizer ground states of general Hamiltonians

In this section, we present the equivalence between the stabilizer ground state and the restricted maximally-commuting Pauli subset of any Hamiltonian. Furthermore, we show that, for properly defined sparse Hamiltonian (which includes almost all common Hamiltonians), such equivalence implies a much cheaper algorithm to get the stabilizer state compared with the brute-force approach. We first define the stabilizer ground state of Hamiltonian H :

Definition 1. *The stabilizer ground state of a given Hamiltonian H is the stabilizer state $|\psi\rangle$ with the lowest energy expectation $\langle\psi|H|\psi\rangle$.*

The number of n -qubit stabilizer states is $\mathcal{S}(n) = 2^n \prod_{i=1}^n (2^i + 1) \sim 2^{\frac{1}{2}(n+1)(n+2)}$, thus looping over all the stabilizer states is infeasible for large n [51]. To find the stabilizer ground state, Lemma 1 is first presented to determine the expectation value of a Pauli operator in a stabilizer state:

Lemma 1. *For any n -qubit stabilizer state $|\psi\rangle$ and Pauli operator $P \in \mathcal{P}_n$, if $P \notin \pm \text{Stab}(|\psi\rangle)$, then $\langle \psi | P | \psi \rangle = 0$*

Proof. Since $\text{Stab}(|\psi\rangle)$ is a full stabilizer group, there exists $Q \in \text{Stab}(|\psi\rangle)$ such that $\{P, Q\} = 0$. Thus

$$\langle \psi | P | \psi \rangle = \langle \psi | PQ | \psi \rangle = -\langle \psi | QP | \psi \rangle = -\langle \psi | P | \psi \rangle. \quad (1)$$

Therefore, $\langle \psi | P | \psi \rangle = 0$. \square

We further extend the concept of energy expectation associated with a stabilizer state to a (not necessarily full) stabilizer group:

Definition 2. *The energy of a stabilizer group \mathbf{S} for a given Pauli operator P or a Pauli Hamiltonian $H = \sum_{P \in \mathbf{P}} w_P P$ is defined by*

$$\begin{aligned} E_{\text{stab}}(P, \mathbf{S}) &= \begin{cases} \pm 1 & P \in \pm \mathbf{S} \\ 0 & \text{otherwise} \end{cases}, \\ E_{\text{stab}}(H, \mathbf{S}) &= \sum_{P \in \mathbf{P}} w_P E_{\text{stab}}(P, \mathbf{S}). \end{aligned} \quad (2)$$

The relationship of stabilizer state energies and stabilizer group energies can be given by:

Corollary 1. *We denote $\tilde{\mathbf{P}} = \pm \mathbf{P} = \{\pm P | P \in \mathbf{P}\}$ for a set of Pauli operators \mathbf{P} . For a Hamiltonian $H = \sum_{P \in \mathbf{P}} w_P P$ and a stabilizer state $|\psi\rangle$, let stabilizer group $\mathbf{S} = \langle \text{Stab}(|\psi\rangle) \cap \tilde{\mathbf{P}} \rangle$, we have $\langle \psi | H | \psi \rangle = E_{\text{stab}}(H, \mathbf{S})$.*

Corollary 1 implies that, once we find all possible $\mathbf{S} = \langle \text{Stab}(|\psi\rangle) \cap \tilde{\mathbf{P}} \rangle$, \mathbf{S} with the lowest $E_{\text{stab}}(H, \mathbf{S})$ naturally corresponds to the stabilizer ground state (might be degenerate). The concept of restricted commuting Pauli subsets is introduced as follows:

Definition 3. *We define the restricted commuting subsets induced by \mathbf{P} as*

$$\mathcal{S}(\mathbf{P}) = \{\mathbf{Q} \subseteq \tilde{\mathbf{P}} | \mathbf{Q} = \langle \mathbf{Q} \rangle \cap \tilde{\mathbf{P}}, -I \notin \langle \mathbf{Q} \rangle\}, \quad (3)$$

where $-I \notin \langle \mathbf{Q} \rangle$ implicitly indicates that $\langle \mathbf{Q} \rangle$ is a stabilizer group. For any $\mathbf{Q} \in \mathcal{S}(\mathbf{P})$, $\langle \mathbf{Q} \rangle$ is a stabilizer group generated by elements in $\tilde{\mathbf{P}}$.

The condition $\mathbf{Q} = \langle \mathbf{Q} \rangle \cap \tilde{\mathbf{P}}$ is designed to satisfy $\mathbf{S} = \langle \text{Stab}(|\psi\rangle) \cap \tilde{\mathbf{P}} \rangle$ mentioned in Corollary 1. We now present Theorem 1, which states that the stabilizer ground state can be obtained by searching for $\mathbf{Q} \in \mathcal{S}(\mathbf{P})$ with the lowest $E_{\text{stab}}(H, \langle \mathbf{Q} \rangle)$. The proof is given in the Appendix V A.

Theorem 1. *Given a Hamiltonian $H = \sum_{P \in \mathbf{P}} w_P P$, then*

$$E_{\min} = \min_{\mathbf{Q} \in \mathcal{S}(\mathbf{P})} E_{\text{stab}}(H, \langle \mathbf{Q} \rangle) \quad (4)$$

is the stabilizer ground state energy. Such \mathbf{Q} minimizes $E_{\text{stab}}(H, \langle \mathbf{Q} \rangle)$ is named as the **restricted maximally-commuting Pauli subset** of H . Additionally, for any $\mathbf{S} = \langle \mathbf{Q} \rangle$, $\mathbf{Q} \in \mathcal{S}(\mathbf{P})$ such that $E_{\text{stab}}(H, \mathbf{S}) = E_{\min}$, each stabilizer state $|\psi\rangle$ stabilized by \mathbf{S} is a (degenerate) stabilizer ground state.

Theorem 1 suggests that the stabilizer ground state of a Hamiltonian $H = \sum_{P \in \mathbf{P}} w_P P$ can be found by listing all elements of $\mathcal{S}(\mathbf{P})$, and thus the computational cost is scaled with $|\mathcal{S}(\mathbf{P})|$. However, the exact value of $|\mathcal{S}(\mathbf{P})|$ heavily depends on the form of the Hamiltonian, e.g. the commutation/anticommutation relations between the Pauli terms. We give a loose upper bound of $|\mathcal{S}(\mathbf{P})|$ as follows:

Lemma 2. *If \mathbf{P} is defined on at most n qubits, then $|\mathcal{S}(\mathbf{P})| \leq (n+1)|\tilde{\mathbf{P}}|^n$.*

Proof. For any $\mathbf{Q} \in \mathcal{S}(\mathbf{P})$, $\langle \mathbf{Q} \rangle$ is constructed by at most n independent generators in $\tilde{\mathbf{P}}$. We simply select each generator one by one, each with at most $|\tilde{\mathbf{P}}|$ choices. Thus, we have $|\mathcal{S}(\mathbf{P})| \leq \sum_{l=0}^n |\tilde{\mathbf{P}}|^l \leq (n+1)|\tilde{\mathbf{P}}|^n$. \square

In fact, we will see that if $|\mathbf{P}|$ scales polynomial with n , $|\mathcal{S}(\mathbf{P})|$ will have a slower growing rate than the number of n -qubit stabilizer states $\mathcal{S}(n)$. Therefore we define the sparse Hamiltonians as follows:

Definition 4. A n -qubit Pauli Hamiltonian $H = \sum_{P \in \mathbf{P}} w_P P$ is sparse if $|\mathbf{P}| \sim O(\text{poly}(n))$.

We note that almost all the common Hamiltonians are sparse Hamiltonians. Now we estimate $|\mathcal{S}(\mathbf{P})|$ of sparse Hamiltonians:

Corollary 2. For sparse Hamiltonians $H = \sum_{P \in \mathbf{P}} w_P P$, $|\mathcal{S}(\mathbf{P})| \sim \exp(Cn \log n)$ for some constant C .

For sparse Hamiltonians, although $|\mathcal{S}(\mathbf{P})|$ still increases exponentially with n , it is much smaller than the number of n -qubit stabilizer states $\mathcal{S}(n) \sim 2^{\frac{1}{2}(n+1)(n+2)}$. In fact, $|\mathcal{S}(\mathbf{P})| \sim \exp(Cn \log n)$ is also related to the computational scaling of the following algorithm for 1D local Hamiltonians.

C. Stabilizer ground states of 1D local Hamiltonians

In this section, we present an algorithm to determine the stabilizer ground state of a given n -qubit 1D local Hamiltonian with an $O(n)$ computational scaling, i.e., the exact 1D local algorithm. After introducing a few definitions and lemmas, we first outline the scratch strategy with a failed but almost working solution in Sec. II C 1, and then provide the formal and complete solution in Sec. II C 2. We first define a k -local Hamiltonian as:

Definition 5. A Hamiltonian $H = \sum_{P \in \mathbf{P}} w_P P$ is k -local if each $P \in \mathbf{P}$ is between qubit q_P^{first} to q_P^{last} that satisfies $q_P^{\text{last}} - q_P^{\text{first}} \leq k - 1$.

Next, we define the projection operation and the truncation operation as follows:

Definition 6. We denote $\mathcal{P}_{m,l} = \pm\{I_i, X_i, Y_i, Z_i\}_{i=m}^l$, where i indicates the qubit index. The **projection** of a set of Pauli operators \mathbf{P} to qubit $m, m+1, \dots, l$ is $\mathbb{P}_{m,l}(\mathbf{P}) = \mathbf{P} \cap \mathcal{P}_{m,l}$.

Definition 7. Let $P \in \mathcal{P}_n$ be a Pauli operator, and $P = \pm p_1 \otimes p_2 \otimes \dots \otimes p_n$, where $p_i \in \{I, X, Y, Z\}$. The **truncation** of P to qubits $m, m+1, \dots, l$ is $\mathbb{T}_{m,l}(P) = \otimes_{i=m}^l p_i$. Similarly, the truncation of a set of Pauli operators \mathbf{P} is $\mathbb{T}_{m,l}(\mathbf{P}) = \{\mathbb{T}_{m,l}(P) | P \in \mathbf{P}\}$.

We also prove the following lemma, which will be frequently used in presenting the exact 1D local algorithm.

Lemma 3. If $\mathbf{B} \subseteq \mathcal{P}_{m,l}$, then $\mathbb{P}_{m,l}(\langle \mathbf{A}, \mathbf{B} \rangle) = \langle \mathbb{P}_{m,l}(\langle \mathbf{A} \rangle), \mathbf{B} \rangle$.

Proof. We only need to prove $\langle \mathbf{A}, \mathbf{B} \rangle \cap \mathcal{P}_{m,l} = \langle \mathbf{A} \cap \mathcal{P}_{m,l}, \mathbf{B} \rangle$. This can be seen by (1) $\langle \mathbf{A} \cap \mathcal{P}_{m,l}, \mathbf{B} \rangle \subseteq \langle \mathbf{A}, \mathbf{B} \rangle$, (2) $\langle \mathbf{A} \cap \mathcal{P}_{m,l}, \mathbf{B} \rangle \subseteq \mathcal{P}_{m,l}$ since $\mathbf{A} \cap \mathcal{P}_{m,l} \subseteq \mathcal{P}_{m,l}$ and $\mathbf{B} \subseteq \mathcal{P}_{m,l}$, and (3) for any $P = \langle \mathbf{A}, \mathbf{B} \rangle \cap \mathcal{P}_{m,l}$ we can write $P = AB$ where $A \in \mathbf{A}$ and $B \in \mathbf{B}$. Since $B \in \mathcal{P}_{m,l}$, $P \in \mathcal{P}_{m,l}$, we also have $A \in \mathcal{P}_{m,l}$. Thus, $P = AB \in \langle \mathbb{P}_{m,l}(\langle \mathbf{A} \rangle), \mathbf{B} \rangle$. \square

1. Illustration of ideas with failed but almost working solution

In principle, all $\mathbf{Q} \in \mathcal{S}(\mathbf{P}) = \{\mathbf{Q} \subseteq \tilde{\mathbf{P}} | \mathbf{Q} = \langle \mathbf{Q} \rangle \cap \tilde{\mathbf{P}}, -I \notin \langle \mathbf{Q} \rangle\}$ should be looped over to find the stabilizer ground state of an n -qubit Hamiltonian $H = \sum_{P \in \mathbf{P}} w_P P$. As mentioned previously, $\mathcal{S}(\mathbf{P})$ scales exponentially with n . In order to obtain a linearly scaled algorithm, we divide \mathbf{P} to groups by the last non-identity qubit q_P^{last} for any $P \in \mathbf{P}$. As a shorthand, we denote $\mathbf{P}_C = \{P \in \mathbf{P} | \text{condition } C \text{ is satisfied for } q_P^{\text{last}}\}$. For example $\mathbf{P}_m = \{P \in \mathbf{P} | q_P^{\text{last}} = m\}$, and $\mathbf{P}_{<m} = \{P \in \mathbf{P} | q_P^{\text{last}} < m\}$. We also define $\tilde{\mathbf{P}}_C$ in the same way for $\tilde{\mathbf{P}}$. Thus, we have $\tilde{\mathbf{P}} = \cup_{m=1}^n \tilde{\mathbf{P}}_m$. Similarly, we divide $\mathbf{Q} \in \mathcal{S}(\mathbf{P})$ into $\mathbf{Q} = \cup_{m=1}^n \mathbf{Q}_m$ with $\mathbf{Q}_m = \mathbf{Q} \cap \tilde{\mathbf{P}}_m$. Now we sequentially determine the possible values of each \mathbf{Q}_m starting from $m = 0$. At qubit m , we will determine \mathbf{Q}_m given that $\mathbf{Q}_{<m}$ has been determined. We first determine the conditions of \mathbf{Q}_m .

Lemma 4. Let $\mathbf{Q} \subseteq \tilde{\mathbf{P}}$ and $\mathbf{Q}_m = \mathbf{Q} \cap \tilde{\mathbf{P}}_m$. Then $\mathbf{Q} \in \mathcal{S}(\mathbf{P})$ is equivalent to $\mathbf{Q}_{\leq m} \in \mathcal{S}(\mathbf{P}_{\leq m})$ with $0 \leq m \leq n$.

Proof. The necessity can be seen from $\mathbf{Q} = \mathbf{Q}_{\leq n}$. For the sufficiency, we recall that $\mathcal{S}(\mathbf{P}) = \{\mathbf{Q} | \mathbf{Q} = \langle \mathbf{Q} \rangle \cap \tilde{\mathbf{P}}, -I \notin \langle \mathbf{Q} \rangle\}$. Then $-I \notin \langle \mathbf{Q}_{\leq m} \rangle$ is obvious because $\mathbf{Q}_{\leq m} \subseteq \mathbf{Q}$. Given that $\mathbf{Q} = \langle \mathbf{Q} \rangle \cap \tilde{\mathbf{P}}$, we have $\langle \mathbf{Q}_{\leq m} \rangle \cap \tilde{\mathbf{P}}_{\leq m} \subseteq \langle \mathbf{Q} \rangle \cap \tilde{\mathbf{P}}_{\leq m} = \langle \mathbf{Q} \rangle \cap \tilde{\mathbf{P}} \cap \tilde{\mathbf{P}}_{\leq m} = \mathbf{Q} \cap \tilde{\mathbf{P}}_{\leq m} = \mathbf{Q}_{\leq m}$. On the other hand, we must have $\mathbf{Q}_{\leq m} \subseteq \langle \mathbf{Q}_{\leq m} \rangle \cap \tilde{\mathbf{P}}_{\leq m}$. Thus $\langle \mathbf{Q}_{\leq m} \rangle \cap \tilde{\mathbf{P}}_{\leq m} = \mathbf{Q}_{\leq m}$ holds for each m , and thus $\mathbf{Q}_{\leq m} \in \mathcal{S}(\mathbf{P}_{\leq m})$ for each m . \square

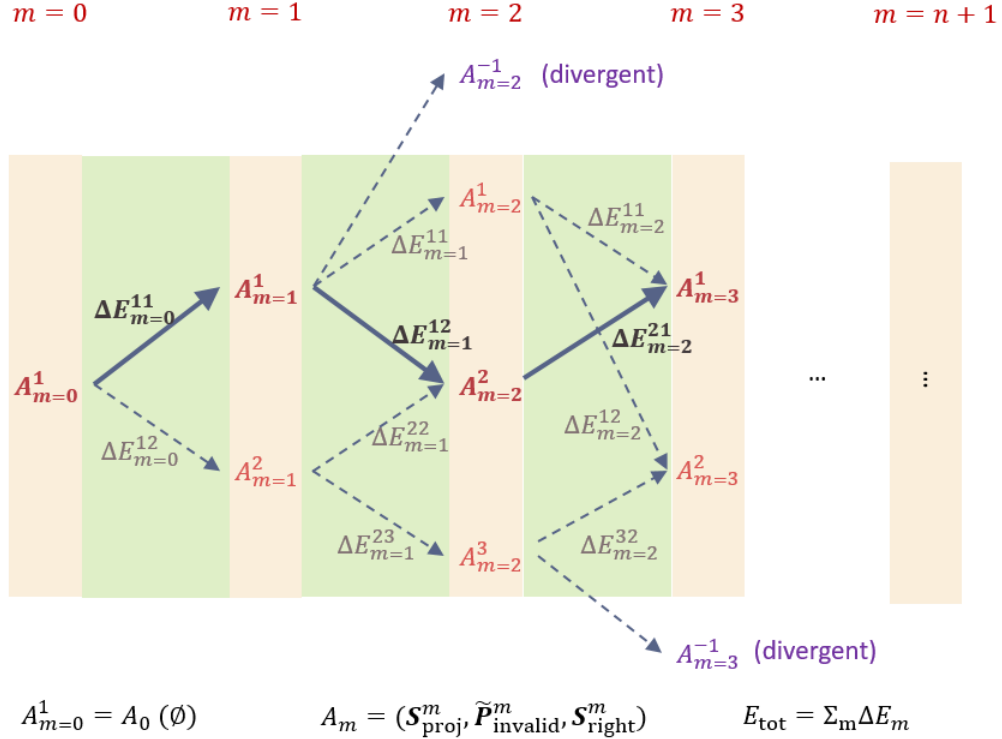


FIG. 1. Schematic diagram of the algorithm to obtain the exact stabilizer ground state of 1D local Hamiltonians. Starting with the initial $A_{m=0} = A_0(\emptyset)$, we sequentially determine the possible values of $A_{m+1} \in F(A_m)$ for each A_m , where $F(A_m)$ is defined in Definition 9. In this process, each A_m can generate multiple A_{m+1} , and each A_{m+1} can be generated from multiple A_m . An energy difference ΔE_m can be determined from each connected pair (A_m, A_{m+1}) . There exists a one-to-one correspondence between each full path $\{A_{m=0}^{n+1}\}$ and $\mathbf{Q} \in \mathcal{S}(\mathbf{P})$. The sum of all the energy differences in the path $\{A_{m=0}^{n+1}\}$ exactly gives the total energy of the stabilizer states stabilized by the corresponding \mathbf{Q} . By sequentially determining the minimum energy $E_{\text{gs}}(A_m)$ on each A_m starting from $m = 0$ via Corollary 3, we can obtain the stabilizer ground state and its energy with an $O(n)$ scaling. Some "divergent branches" A_m (marked in purple) might be created during the whole process. However, these branches do not impact the final results, as they do not connect with any A_{m+1} .

Given $\mathbf{Q}_{<m} \in \mathcal{S}(\mathbf{P}_{<m})$, we say \mathbf{Q}_m is valid to add to $\mathbf{Q}_{<m}$ (or simply \mathbf{Q}_m is valid if there's no ambiguity) if $\mathbf{Q}_{\leq m} \in \mathcal{S}(\mathbf{P}_{\leq m})$. Thus looping over $\mathbf{Q} \in \mathcal{S}(\mathbf{P})$ is equivalent to sequentially find all valid \mathbf{Q}_m from $\mathbf{Q}_{<m}$ with m increasing from 1 to n . However, the number of possible $\mathbf{Q}_{<m}$ increases exponentially with m . In order to ensure the scalability, we define a local state

$$A_m(\mathbf{Q}) = A_m(\mathbf{Q}_{<m}) = (\mathbf{S}_{\text{proj}}^m(\mathbf{Q}_{<m}), \tilde{\mathbf{P}}_{\text{invalid}}^m(\mathbf{Q}_{<m})), \quad (5)$$

where

$$\begin{aligned} \mathbf{S}_{\text{proj}}^m(\mathbf{Q}_{<m}) &= \mathbb{P}_{m-k+1, m-1}(\langle \mathbf{Q}_{<m} \rangle) \\ \tilde{\mathbf{P}}_{\text{invalid}}^m(\mathbf{Q}_{<m}) &= \{P \in \tilde{\mathbf{P}}_{\geq m} \mid [P, \mathbf{Q}_{<m}] \neq 0\}. \end{aligned} \quad (6)$$

The locality of $\mathbf{S}_{\text{proj}}^m$ is clear, and meanwhile the locality of $\tilde{\mathbf{P}}_{\text{invalid}}^m$ can be observed by $[P, \mathbf{Q}_{<m}] = 0$ for any $q_P^{\text{last}} \geq m + k - 1$. The following claim is desired to hold for $A_m = (\mathbf{S}_{\text{proj}}^m, \tilde{\mathbf{P}}_{\text{invalid}}^m)$:

Claim 1. For any $\mathbf{Q}_{<m} \in \mathcal{S}(\mathbf{P}_{<m})$, $A_m(\mathbf{Q}_{<m})$ can accomplish the following tasks without the knowledge of $\mathbf{Q}_{<m}$:

1. determine $A_{m+1}(\mathbf{Q}_{<m+1})$ given a valid \mathbf{Q}_m , where $\mathbf{Q}_{<m+1} = \mathbf{Q}_{<m} \cup \mathbf{Q}_m$
2. determine whether a given $\mathbf{Q}_m \subseteq \tilde{\mathbf{P}}_m$ is valid to add to $\mathbf{Q}_{<m}$

If Claim 1 holds, we can then construct a map from each A_m to a set of A_{m+1} generated from A_m with all valid values of \mathbf{Q}_m :

$$F(A_m) = \{A_{m+1}(A_m, \mathbf{Q}_m) \mid \text{valid } \mathbf{Q}_m\}. \quad (7)$$

For compatibility with the formal solution in Sec. II C 2, we provide a more general definition of F as

$$F(A_m) = \{A_{m+1}(\mathbf{Q}) | \mathbf{Q} \in \mathcal{S}(\mathbf{P}), A_m = A_m(\mathbf{Q})\}. \quad (8)$$

The function F can be interpreted as the transition function in the automata theory [52, 53].

Now we consider stabilizer group energies $E_{\text{stab}}(H, \langle \mathbf{Q}_{<m} \rangle)$. According to $\langle \mathbf{Q}_{<m+1} \rangle \cap \tilde{\mathbf{P}} = \mathbf{Q}_{<m+1}$ and $\langle \mathbf{Q}_{<m} \rangle \cap \tilde{\mathbf{P}} = \mathbf{Q}_{<m}$, the energy difference between $\langle \mathbf{Q}_{<m+1} \rangle$ and $\langle \mathbf{Q}_{<m} \rangle$ is fully determined by $\mathbf{Q}_m \subseteq \tilde{\mathbf{P}}_m = \pm \mathbf{P}_m$ as

$$\begin{aligned} \Delta E(\mathbf{Q}_m) &= E_{\text{stab}}(H, \langle \mathbf{Q}_{<m+1} \rangle) - E_{\text{stab}}(H, \langle \mathbf{Q}_{<m} \rangle) \\ &= \sum_{Q \in \mathbf{Q}_m \cap \mathbf{P}_m} w_Q - \sum_{Q \in \mathbf{Q}_m \cap (-\mathbf{P}_m)} w_{-Q}. \end{aligned} \quad (9)$$

However, \mathbf{Q}_m cannot be uniquely determined by A_m and $A_{m+1} \in F(A_m)$, thus we define the list of possible \mathbf{Q}_m as

$$V(A_m, A_{m+1}) = \{\mathbf{Q}_m | A_{m+1} = A_{m+1}(A_m, \mathbf{Q}_m)\}. \quad (10)$$

Starting from $A_0 = A_0(\emptyset)$, we can then efficiently find all possible A_m with m increasing from 0 to $n + 1$. If we additionally record the minimal energy for each A_m (will be defined soon), we can then obtain the stabilizer ground state and its energy of a given Hamiltonian H . Since A_m only contains local information, the number of possible A_m is up to a constant agnostic to the system size. Therefore, the total cost is linear to the number of qubits n . Formally we define:

Definition 8. *The stabilizer ground state and its energy for A_m are defined as*

$$\begin{aligned} \mathbf{S}_{\text{gs}}(A_m) &= \langle \mathbf{Q}'_{<m} \rangle \\ E_{\text{gs}}(A_m) &= E_{\text{stab}}(H, \langle \mathbf{Q}'_{<m} \rangle) \end{aligned} \quad (11)$$

with $\mathbf{Q}'_{<m} = \mathbf{Q}' \cap \tilde{\mathbf{P}}_{<m}$, where

$$\mathbf{Q}' = \arg \min_{\mathbf{Q} \in \mathcal{S}(\mathbf{P}): A_m = A_m(\mathbf{Q})} E_{\text{stab}}(H, \langle \mathbf{Q}_{<m} \rangle). \quad (12)$$

According to the expression between the energy difference of $\langle \mathbf{Q}_{<m+1} \rangle$ and $\langle \mathbf{Q}_{<m} \rangle$ given in Eq. (9), the values of $E_{\text{gs}}(A_{m+1})$ and $\mathbf{S}_{\text{gs}}(A_{m+1})$ can be derived from $E_{\text{gs}}(A_m)$ and $\mathbf{S}_{\text{gs}}(A_m)$ as:

$$\begin{aligned} E_{\text{gs}}(A_{m+1}) &= E_{\text{gs}}(A'_m) + \Delta E(\mathbf{Q}'_m) \\ \mathbf{S}_{\text{gs}}(A_{m+1}) &= \langle \mathbf{S}_{\text{gs}}(A'_m), \mathbf{Q}'_m \rangle, \end{aligned} \quad (13)$$

where

$$(A'_m, \mathbf{Q}'_m) = \arg \min_{A_m, \mathbf{Q}_m: A_{m+1} \in F(A_m), \mathbf{Q}_m \in V(A_m, A_{m+1})} E(A_m) + \Delta E(\mathbf{Q}_m). \quad (14)$$

Once $F(A_m)$ satisfies Eq. (8), the stabilizer ground state can be obtained by:

Corollary 3. *Assume function F satisfies Eq. (8). Starting from $A_0 = A_0(\emptyset)$, $E_{\text{gs}}(A_0) = 0$, $\mathbf{S}(A_0) = \langle \emptyset \rangle$, all values of A_{n+1} and the corresponding $(E_{\text{gs}}(A_{n+1}), \mathbf{S}_{\text{gs}}(A_{n+1}))$ can be generated by sequentially applying $A_{m+1} \in F(A_m)$ and Eq. 13. The stabilizer ground state of H is given by $\mathbf{S}_{\text{gs}} = \mathbf{S}_{\text{gs}}(A'_{n+1})$ and $E_{\text{gs}} = E_{\text{gs}}(A'_{n+1})$, where*

$$A'_{n+1} = \arg \min_{A_{n+1}} E_{\text{gs}}(A_{n+1}), \quad (15)$$

As long as the corresponding function F exists, Corollary 3 provides the algorithm to obtain stabilizer ground states of 1D local Hamiltonians with $O(n)$ scaling.

Finally, we consider whether Claim 1 holds for A_m . Firstly, we consider the expression of $A_{m+1}(A_m, \mathbf{Q}_m)$ for a valid \mathbf{Q}_m . $A_{m+1} = (\mathbf{S}_{\text{proj}}^{m+1}, \tilde{\mathbf{P}}_{\text{invalid}}^{m+1})$ is given by

$$\begin{aligned} \mathbf{S}_{\text{proj}}^{m+1} &= \mathbb{P}_{m-k+2, m}(\langle \mathbf{Q}_{<m}, \mathbf{Q}_m \rangle) \\ &= \mathbb{P}_{m-k+2, m}(\mathbb{P}_{m-k+1, m}(\langle \mathbf{Q}_{<m}, \mathbf{Q}_m \rangle)) \\ &= \mathbb{P}_{m-k+2, m}(\langle \mathbb{P}_{m-k+1, m}(\langle \mathbf{Q}_{<m} \rangle), \mathbf{Q}_m \rangle) \\ &= \mathbb{P}_{m-k+2, m}(\langle \mathbf{S}_{\text{proj}}^m, \mathbf{Q}_m \rangle), \end{aligned} \quad (16)$$

where Lemma 3 is applied in the third line, and

$$\begin{aligned}\tilde{\mathbf{P}}_{\text{invalid}}^{m+1} &= \{P \in \tilde{\mathbf{P}}_{\geq m+1} \mid [P, \mathbf{Q}_{<m+1}] \neq 0\} \\ &= \{P \in \tilde{\mathbf{P}}_{\geq m+1} \mid P \in \tilde{\mathbf{P}}_{\text{invalid}}^m \text{ or } [P, \mathbf{Q}_m] \neq 0\}.\end{aligned}\quad (17)$$

In the following, the Eq. (16) and Eq. (17) are abbreviated as $\mathbf{S}_{\text{proj}}^{m+1}(\mathbf{S}_{\text{proj}}^m, \mathbf{Q}_m)$ and $\tilde{\mathbf{P}}_{\text{invalid}}^{m+1}(\tilde{\mathbf{P}}_{\text{invalid}}^m, \mathbf{Q}_m)$, respectively.

Secondly, we consider how to determine whether a given \mathbf{Q}_m is valid. The validity of \mathbf{Q}_m can be simplified as follows:

Corollary 4. *Given $\mathbf{Q}_{\leq i} \in \mathcal{S}(\mathbf{P}_{\leq i})$ for $i < m$, \mathbf{Q}_m is valid if and only if*

1. $\langle \mathbf{Q}_m \rangle$ is a stabilizer group, i.e. $[P, Q] = 0$ for $P, Q \in \mathbf{Q}_m$ and $-I \notin \langle \mathbf{Q}_m \rangle$.
2. $[\mathbf{Q}_m, \mathbf{Q}_{<m}] = 0$.
3. $\langle \mathbf{Q}_{<m}, \mathbf{Q}_m \rangle \cap \tilde{\mathbf{P}}_m = \mathbf{Q}_m$.
4. $\langle \mathbf{Q}_{<m}, \mathbf{Q}_m \rangle \cap \tilde{\mathbf{P}}_{<m} = \mathbf{Q}_{<m}$.

The first condition can be determined by checking \mathbf{Q}_m itself, and the second condition is equivalent to $\mathbf{Q}_m \cap \tilde{\mathbf{P}}_{\text{invalid}}^m = \emptyset$. The third condition is equivalent to $\langle \mathbf{S}_{\text{proj}}^m, \mathbf{Q}_m \rangle \cap \tilde{\mathbf{P}}_m = \mathbf{Q}_m$ derived from

$$\begin{aligned}\langle \mathbf{Q}_{<m}, \mathbf{Q}_m \rangle \cap \tilde{\mathbf{P}}_m &= \mathbb{P}_{m-k+1,m}(\langle \mathbf{Q}_{<m}, \mathbf{Q}_m \rangle) \cap \tilde{\mathbf{P}}_m \\ &= \langle \mathbb{P}_{m-k+1,m}(\langle \mathbf{Q}_{<m} \rangle), \mathbf{Q}_m \rangle \cap \tilde{\mathbf{P}}_m \\ &= \langle \mathbf{S}_{\text{proj}}^m, \mathbf{Q}_m \rangle \cap \tilde{\mathbf{P}}_m.\end{aligned}\quad (18)$$

However, the definition of $A_m = (\mathbf{S}_{\text{proj}}^m, \tilde{\mathbf{P}}_{\text{invalid}}^m)$ is not sufficient to determine whether the last condition in Corollary 4 is satisfied or not. An example is $\mathbf{P} = \{X_1, X_1X_2, X_2X_3, X_3\}$ and $k = 2$. In case of $\mathbf{Q}_1 = \{X_1\}$ and $\mathbf{Q}_2 = \emptyset$, we have $\mathbf{S}_{\text{proj}}^3 = \langle \emptyset \rangle$ and $\tilde{\mathbf{P}}_{\text{invalid}}^3 = \emptyset$, which should allow the choice of $\mathbf{Q}_3 = \{X_2X_3, X_3\}$. However, $\mathbf{Q} = \{X_1, X_2X_3, X_3\}$ does not satisfy $\langle \mathbf{Q} \rangle \cap \tilde{\mathbf{P}} = \mathbf{Q}$ (because $X_1X_2 = X_1 \cdot X_2X_3 \cdot X_3$). Therefore, we conclude that A_m defined in Eq. (5) does not satisfy Claim 1, and thus cannot provide the function $F(A_m)$ satisfying the condition in Eq. (8). The approach to closing this loophole and the final complete formalism is further discussed in Section II C 2.

2. Formal solution

In Sec II C 1, we have discussed how the exact 1D local algorithm can be obtained via Corollary 3 once a suitable local state A_m and its corresponding transition function F are identified. However, the naive definition of A_m in Eq. (5) fails to yield an F satisfying Eq. (8) due to the lack of ability to verify the validity of a given \mathbf{Q}_m . In order to fix this issue, we propose

$$\mathbf{S}_{\text{right}}^m(\mathbf{Q}_{\geq m}) = \mathbb{P}_{m-k+1,m}(\langle \mathbf{Q}_{\geq m} \rangle), \quad (19)$$

which is a stabilizer group in $\mathcal{P}_{m-k+1,m}$. Unlike $\mathbf{S}_{\text{proj}}^m$ and $\tilde{\mathbf{P}}_{\text{invalid}}^m$ introduced previously, which are functions of $\mathbf{Q}_{<m}$, $\mathbf{S}_{\text{right}}^m$ is a function of $\mathbf{Q}_{\geq m}$, which is unknown until we obtain \mathbf{Q}_m for all m . Consequently, $\mathbf{S}_{\text{right}}^m$ should be treated as a “preclaimed” attribute of the yet-to-be-determined $\mathbf{Q}_{\geq m}$, rather than as a component of the local state A_m for validating \mathbf{Q}_m . We start by demonstrating that $\mathbf{S}_{\text{right}}^m$ fully determines \mathbf{Q}_m in the following lemma:

Lemma 5. *If $\mathbf{Q} \in \mathcal{S}(\mathbf{P})$, then $\mathbf{S}_{\text{right}}^m(\mathbf{Q}_{\geq m}) \cap \tilde{\mathbf{P}}_m = \mathbf{Q}_m$.*

Proof. On one hand, we have $\mathbf{Q}_m \subseteq \tilde{\mathbf{P}}_m$ and $\mathbf{Q}_m = \mathbb{P}_{m-k+1,m}(\mathbf{Q}_m) \subseteq \mathbb{P}_{m-k+1,m}(\langle \mathbf{Q}_{\geq m} \rangle) = \mathbf{S}_{\text{right}}^m(\mathbf{Q}_{\geq m})$, thus $\mathbf{Q}_m \subseteq \mathbf{S}_{\text{right}}^m(\mathbf{Q}_{\geq m}) \cap \tilde{\mathbf{P}}_m$. On the other hand, we have $\mathbf{S}_{\text{right}}^m(\mathbf{Q}_{\geq m}) = \mathbb{P}_{m-k+1,m}(\langle \mathbf{Q}_{\geq m} \rangle) \subseteq \langle \mathbf{Q} \rangle$, thus $\mathbf{S}_{\text{right}}^m(\mathbf{Q}_{\geq m}) \cap \tilde{\mathbf{P}}_m \subseteq \langle \mathbf{Q} \rangle \cap \tilde{\mathbf{P}}_m = (\langle \mathbf{Q} \rangle \cap \tilde{\mathbf{P}}) \cap \tilde{\mathbf{P}}_m = \mathbf{Q}_m$. Combining the above two conclusions results in $\mathbf{S}_{\text{right}}^m(\mathbf{Q}_{\geq m}) \cap \tilde{\mathbf{P}}_m = \mathbf{Q}_m$. \square

Lemma 5 allows us to shift the problem from “searching for valid \mathbf{Q}_m ” to “searching for $\mathbf{S}_{\text{right}}^m$ to make $\mathbf{Q}_m = \mathbf{S}_{\text{right}}^m \cap \tilde{\mathbf{P}}_m$ valid” instead. Once a valid $\mathbf{S}_{\text{right}}^m$ and consequently a valid \mathbf{Q}_m , is identified, we can similarly update $\mathbf{S}_{\text{proj}}^m$ and $\tilde{\mathbf{P}}_{\text{invalid}}^m$ by $\mathbf{S}_{\text{proj}}^{m+1} = \mathbf{S}_{\text{proj}}^{m+1}(\mathbf{S}_{\text{proj}}^m, \mathbf{Q}_m)$ and $\tilde{\mathbf{P}}_{\text{invalid}}^{m+1} = \tilde{\mathbf{P}}_{\text{invalid}}^{m+1}(\tilde{\mathbf{P}}_{\text{invalid}}^m, \mathbf{Q}_m)$ as defined in Eq. (16) and (17).

To outline how the introduction of $\mathbf{S}_{\text{right}}^m$ addresses the existing issue, we revisit the previous example $\mathbf{P} = \{X_1, X_1X_2, X_2X_3, X_3\}$, $k = 2$, with fixed $\mathbf{Q}_1 = \{X_1\}$ and $\mathbf{Q}_2 = \emptyset$. Without the knowledge of $\mathbf{S}_{\text{right}}^{m=2}$, $\mathbf{Q}_3 = \{X_2X_3, X_3\}$ is an allowed choice, since the only information provided at $m = 3$ is $\mathbf{S}_{\text{proj}}^{m=3} = \langle \mathbf{Q}_2 \rangle$. However, if we require the knowledge of $\mathbf{S}_{\text{right}}^{m=2} = \mathbb{P}_{1,2}(\langle \mathbf{Q}_2, \mathbf{Q}_3 \rangle)$ at $m = 2$, we can immediately exclude the possibility of $\mathbf{Q}_3 = \{X_2X_3, X_3\}$, since it gives $\mathbf{S}_{\text{right}}^{m=2} = \langle X_2 \rangle$ which is invalid.

Since $\mathbf{S}_{\text{right}}^m$ is a “preclaimed property” of the yet-to-be-determined $\langle \mathbf{Q}_{\geq m} \rangle$, it’s crucial to preserve this information as we proceed from A_m to A_{m+1} to ensure it can be fulfilled later. Thus, we integrate $\mathbf{S}_{\text{right}}^m$ as an additional component of A_m , and the formal definition of the local state A_m becomes:

$$A_m = (\mathbf{S}_{\text{proj}}^m, \tilde{\mathbf{P}}_{\text{invalid}}^m, \mathbf{S}_{\text{right}}^m), \quad (20)$$

and the information of $\mathbf{S}_{\text{right}}^m$ is passed into $\mathbf{S}_{\text{right}}^{m+1}$ when we proceed from A_m to A_{m+1} . Similar to Sec. II C 1, given a valid state A_m , our goal is to identify a set of $\{A_{m+1}\} = F(A_m)$ with valid values of $\mathbf{S}_{\text{right}}^{m+1}$. Such function $F(A_m)$ is now defined as follows:

Definition 9. We define $F(A_m)$, which generates branches of $A_{m+1} = (\mathbf{S}_{\text{proj}}^{m+1}, \tilde{\mathbf{P}}_{\text{invalid}}^{m+1}, \mathbf{S}_{\text{right}}^{m+1})$ from a given $A_m = (\mathbf{S}_{\text{proj}}^m, \tilde{\mathbf{P}}_{\text{invalid}}^m, \mathbf{S}_{\text{right}}^m)$, as follows:

1. $\mathbf{S}_{\text{proj}}^{m+1} = \mathbf{S}_{\text{proj}}^{m+1}(\mathbf{S}_{\text{proj}}^m, \mathbf{Q}_m)$ and $\tilde{\mathbf{P}}_{\text{invalid}}^{m+1} = \tilde{\mathbf{P}}_{\text{invalid}}^{m+1}(\tilde{\mathbf{P}}_{\text{invalid}}^m, \mathbf{Q}_m)$ with expressions given in Eq. (16) and (17), where $\mathbf{Q}_m = \mathbf{S}_{\text{right}}^m \cap \tilde{\mathbf{P}}_m$.
2. Create branches of A_{m+1} for each stabilizer group $\mathbf{S}_{\text{right}}^{m+1} \subseteq \mathcal{P}_{m-k+2, m+1}$ that satisfies:
 - (a) $\mathbf{Q}_{m+1} = \mathbf{S}_{\text{right}}^{m+1} \cap \tilde{\mathbf{P}}_{m+1}$ satisfies the first three conditions of Corollary 4
 - (b) $\mathbf{S}_{\text{right}}^{m+1} \in \mathcal{S}(\mathbb{T}_{m-k+2, m+1}(\tilde{\mathbf{P}}_{\geq m+1} - \tilde{\mathbf{P}}_{\text{invalid}}^{m+1}))$
 - (c) $\langle \mathbf{S}_{\text{proj}}^{m+1}, \mathbf{S}_{\text{right}}^{m+1} \rangle \cap \tilde{\mathbf{P}}_{m+1} = \mathbf{Q}_{m+1}$
 - (d) $\langle \mathbb{P}_{m-k+1, m}(\mathbf{S}_{\text{right}}^{m+1}), \mathbf{Q}_m \rangle = \mathbf{S}_{\text{right}}^m$

In Appendix V B, we prove that, by such construction, $\mathbf{Q}_m = \mathbf{S}_{\text{right}}^m \cap \tilde{\mathbf{P}}_m$ is always valid to be added to $\mathbf{Q}_{<m}$. In Appendix V C, we further prove the one-to-one correspondence between $\{A_{i=0}^{n+1}\}$ generated by F and $\mathbf{Q} \in \mathcal{S}(\mathbf{P})$, i.e., each path $\{A_{i=0}^{n+1}\}$ satisfying $A_0 = A_0(\emptyset)$ and $A_{m+1} \in F(A_m)$ is exactly some $\{A_{i=0}^{n+1}(\mathbf{Q} \in \mathcal{S}(\mathbf{P}))\}$, and vice versa, where $A_m(\mathbf{Q})$ is naturally defined as

$$A_m(\mathbf{Q}) = (\mathbf{S}_{\text{proj}}^m(\mathbf{Q}_{<m}), \tilde{\mathbf{P}}_{\text{invalid}}^m(\mathbf{Q}_{<m}), \mathbf{S}_{\text{right}}^m(\mathbf{Q}_{\geq m})). \quad (21)$$

We note that some A_m may result in $F(A_m) = \emptyset$, which indicates that the “preclaimed” $\mathbf{S}_{\text{right}}^m$ can never be satisfied, and thus no $A_{m+1} \in F(A_m)$ can be found. Those branches A_m that cannot reach $m = n + 1$ are called “divergent branches”. Thus the above one-to-one correspondence is restricted to the full path $\{A_{i=0}^{n+1}\}$ so that these “divergent branches” are excluded. The automaton structure of the local states A_m and the transition function F is visualized in Fig. 1.

The last question to address before employing Corollary 3 is the determination of \mathbf{Q}_m from A_m and A_{m+1} . Different from the failed solution given in Sec. II C 1, this question is trivial now since \mathbf{Q}_m is directly given by A_m , as stated in Lemma 5. To preserve the form of Eq. (13) and (14), we can effectively define

$$V(A_m, A_{m+1}) = V(A_m) = \{\mathbf{S}_{\text{right}}^m \cap \tilde{\mathbf{P}}_m\}. \quad (22)$$

With the above definitions of A_m and F , it is ready for us to derive the exact 1D local algorithm:

Theorem 2. With the local state A_m defined in Eq. (20) and the function $F(A_m)$ defined in Definition 9, Corollary 3 provides the exact algorithm to identify the stabilizer ground state of a given 1D local Hamiltonian.

Proof. We prove that, if we exclude the “divergent branches”, F satisfies the condition in Eq. (8), and consequently the stabilizer ground state of any given 1D local Hamiltonian can be obtained by applying Corollary 3. Furthermore, including such divergent branches is proved to not affect the final results, thus Corollary 3 combined with F itself is sufficient to give the stabilizer ground state.

We first strictly define a function F' , designed to filter out the divergent outcomes produced by F , as:

$$F'(A_m) = \{A_{m+1} \in F(A_m) \mid \exists \{A_{i=m+1}^{n+1}\} \text{ s.t. } A_{i+1} \in F(A_i), m+1 \leq i \leq n\}. \quad (23)$$

Schematically F' can be interpreted as F defined in the central region illustrated in Fig. 1. According to the previous conclusion of the one-to-one correspondence between $\{A_{i=0}^{n+1} \mid A_0 = A_0(\emptyset), A_{m+1} \in F(A_m)\}$ and $\{A_{i=0}^{n+1} \mid Q \in \mathcal{S}(\mathbf{P})\}$, we immediately conclude that F' satisfies the condition in Eq. (8), and thus Corollary 3 with F gives the stabilizer ground state.

Now we show that F provides exactly the same result with F' . Let A_m be a “convergent branch”, i.e., there exists an $\{A_{i=m}^{n+1}\}$ such that $A_{i+1} \in F(A_i)$, $m \leq i \leq n$. The only situation in which F differs from F' is when F generates a “divergent branch” $A_{m+1} \in F(A_m)$, while F' does not. However, such an A_{m+1} would never generate any “convergent branch” $A_{m'}$ with $m' > m+1$ via F . Otherwise, a path $\{A_{i=m+1}^{n+1}\}$ could be generated by F , contradicting to the assumption that A_{m+1} is a “divergent branch”. Thus replacing F' by F does not change the value of $E_{\text{gs}}(A_m)$ and $\mathbf{S}_{\text{gs}}(A_m)$ defined in Definition 8 as long as A_m is a “convergent branch”. Finally, we naturally conclude that Corollary 3 combined with F correctly gives the stabilizer ground state. \square

We additionally comment that the automaton structure shown in Fig. 1 can potentially be applied to different tasks, such as determining excited states and performing thermal state sampling.

Finally, we estimate the computational scaling of the exact 1D local algorithm. We start by considering the number of possible A_m generated from F and $A_0 = A_0(\emptyset)$. However, it does not have a simple expression due to the similar reason mentioned in Sec. II B. A loose upper bound is provided in the following and its detailed proof is given in Appendix V D.

Lemma 6. *Let $H = \sum_{P \in \mathbf{P}} w_P P$ be a k -local Hamiltonian, and there exists M such that $|\mathbf{P}_m| \leq M$ for each m . For any m , $N_A < (4kM)^{3k} = \exp(3k \log 4kM)$ candidate values of A_m could be created solely from $\mathbb{T}_{m-2k+2, m}(\tilde{\mathbf{P}})$, and each A_m generated by F and $A_0 = A_0(\emptyset)$ must be one of these candidates.*

We rewrite $N_A \sim O(\exp(Ck \log kM))$ with some constant C for simplicity and further analysis. The total computational complexity is discussed using this expression as follows. The total cost spent on each qubit m is bounded by the product of (1) the number of A_m , (2) the number of A_{m+1} , and (3) time to compute a single A_{m+1} from a single A_m . Since all stabilizer state operations used in the algorithm can be realized in polynomial scaling of k , the total cost $T \sim n \times O(\exp(Ck \log kM)) \times O(\exp(Ck \log kM)) \times O(\text{poly}(k)) \sim O(n \exp(C'k \log kM))$ with some constant C' .

Similar to Sec. II B, we consider the 1D local and sparse Hamiltonians defined as follows:

Definition 10. *For a 1D k -local Pauli Hamiltonian $H = \sum_{P \in \mathbf{P}} w_P P$, we say that it is sparse if $|\mathbf{P}_m| \sim O(\text{poly}(k))$.*

The conclusions $T \sim O(n \exp(C'k \log kM))$ and $M \sim O(\text{poly}(k))$ lead to the final computation complexity as:

Corollary 5. *The total computational cost T to obtain the stabilizer ground state for a n -qubit, k -local and sparse Hamiltonian satisfies $T \sim O(n \exp(Ck \log k))$ for some constant C .*

D. Stabilizer ground states of infinite periodic Hamiltonians

In this section, we discuss the stabilizer ground state problem of infinite periodic Hamiltonians (referred to as periodic Hamiltonians). We will show that, for any 1D periodic local Hamiltonian, the stabilizer ground state also have periodic stabilizers, but probably with a larger period. Based on the idea of the exact 1D local algorithm presented in Sec. II C, we present an exact algorithm for 1D periodic local Hamiltonians, namely, the exact 1D periodic local algorithm, which scales with $O(l)$, where l is the space translation period. For general periodic Hamiltonians in higher dimensions, we speculate that the stabilizer ground states should still have periodic stabilizers. With this assumption, the formalism in Sec. II B is extended to general periodic Hamiltonians and the equivalence between the stabilizer ground state and the restricted maximally-commuting periodic Pauli subset is also derived.

We first review the properties of the eigenstates of periodic Hamiltonians on an infinitely long 1D lattice. Let T be an operator to translate a given $|\psi\rangle$ by some fixed number of sites, and H be a Hamiltonian satisfying $[H, T] = 0$. Bloch's theorem [54] states that the eigenstates $|\psi\rangle$ of H can be classified by the eigenvalue of T via $T|\psi\rangle = e^{i\phi}|\psi\rangle$ since H and T can be simultaneously diagonalized. In numerical treatments, a supercell with size L is usually introduced and ϕ can take discrete values $\phi = 2\pi \frac{j}{L}$ for integers $0 \leq j < L$ [55, 56].

Now we consider stabilizer states in the qubit space. Let T_l be the operator to translate qubit q to $q + l$ for any q . A Hamiltonian $H = \sum_{P \in \mathbf{P}} w_P P$ is defined to be invariant under T_l if $P' = T_l^\dagger P T_l$ satisfies $P' \in \mathbf{P}$ and $w_{P'} = w_P$ for any $P \in \mathbf{P}$. However, the stabilizer ground state $|\psi\rangle$ of H might not be an eigenstate of T_l , i.e.,

$T_l|\psi\rangle = \lambda|\psi\rangle$ for some λ . An example is $H = H_0 + \epsilon H_I$, where $H_0 = -\sum_n (X_{3n}X_{3n+1}X_{3n+2} + Z_{3n}Z_{3n+1}Z_{3n+2})$ and $H_I = -\sum_n (Z_{3n-1}X_{3n} + X_{3n-1}Z_{3n})$, and H thus has a period of 3. At $\epsilon = 0$, H can be divided into independent subsystems $\{3n, 3n+1, 3n+2\}$ for each n , and each subsystem has degenerate stabilizer ground states with stabilizers $X_{3n}X_{3n+1}X_{3n+2}$ and $Z_{3n}Z_{3n+1}Z_{3n+2}$, respectively. At $0 < \epsilon \ll 1$, the interaction term H_I breaks the degeneracy, and the stabilizers of the stabilizer ground state become alternating $X_{3n}X_{3n+1}X_{3n+2}$ and $Z_{3n}Z_{3n+1}Z_{3n+2}$. This system has a period of 6 and thus does not satisfy $T_{l=3}|\psi\rangle = \lambda|\psi\rangle$.

Theorem 3 states that the stabilizer ground state of a 1D periodic local Hamiltonian can be determined by a relaxed condition $T_{cl}|\psi\rangle = |\psi\rangle$ for some integer c , where c can be interpreted as the supercell size. The proof is given in Appendix V E.

Theorem 3. *Any 1D periodic local Hamiltonian H satisfying $[H, T_l] = 0$ has at least one degenerate stabilizer ground state $|\psi\rangle$ with $T_{cl}|\psi\rangle = |\psi\rangle$ for some integer $c \leq N_A$, where N_A is defined in Lemma 6. Let $\mathbf{S} = \langle \mathbf{Q} \rangle$ with $\mathbf{Q} \in \mathcal{S}(\mathbf{P})$ be the stabilizer group of the corresponding stabilizer ground state. We have $A_m(\mathbf{Q}) = A_{m+cl}(\mathbf{Q})$ for any m .*

Theorem 3 proves a very loose upper bound of the supercell size c , but the actual supercell size might be small (e.g. $c = 1$ or $c = 2$) for physically reasonable Hamiltonians. A linear-scaled algorithm to find the stabilizer ground state of 1D periodic local Hamiltonian H thus can be derived according to Theorem 3:

Corollary 6. *Let H be a 1D periodic local Hamiltonian satisfying $[H, T_l] = 0$. Let \mathbf{A}_l be the set of possible values of A_{m+jl} generated from $A_0 = A_0(\emptyset)$ for integer j . According to Lemma 6 we have $|\mathbf{A}_l| \leq N_A$. Similar to Definition 8, for arbitrary $A_0 \in \mathbf{A}_l$ we define $E_{gs}(A_m; A_0)$ and $\mathbf{S}_{gs}(A_m; A_0)$ by initial values $E_{gs}(A_0; A_0) = 0$ and the same evolution rules from m to $m+1$ in Eq. (13). The stabilizer ground state of H and its energy in a supercell is given by*

$$\begin{aligned} E_{gs} &= E_{gs}(A_{c'l} = A'; A_0 = A') \\ \mathbf{S}_{gs} &= \mathbf{S}_{gs}(A_{c'l} = A'; A_0 = A') \end{aligned} \quad (24)$$

with

$$(c', A') = \arg \min_{c, A \in \mathbf{A}_l} E_{gs}(A_{cl} = A; A_0 = A). \quad (25)$$

The algorithm stated in Theorem 3 is referred to as the exact 1D periodic local algorithm. We then move on to discuss higher-dimensional Hamiltonians. Although it can not be theoretically derived from Theorem 3 that the stabilizer ground state $|\psi\rangle$ satisfies $T_{cl}|\psi\rangle = |\psi\rangle$ for translation operators T_{cl} in each dimension, we speculate that at least some approximated (if not exact) stabilizer ground state satisfies such condition due to its similarity to the supercell treatments of exact eigenstates.

With the assumption of $T_{cl}|\psi\rangle = |\psi\rangle$, we present the stabilizer ground state theory for general infinite periodic Hamiltonians. For any stabilizer P with $P|\psi\rangle = |\psi\rangle$, let $P' = T_{cl}^\dagger P T_{cl}$, we have $P'|\psi\rangle = |\psi\rangle$, and thus P' is also a stabilizer of $|\psi\rangle$. We only need to consider those $\mathbf{Q} \in \mathcal{S}(\mathbf{P})$ such that $\mathbf{Q} = T_{cl}^\dagger Q T_{cl}$. Strictly, we define

$$\mathcal{S}_c(\mathbf{P}) = \{\mathbf{Q} \subseteq \tilde{\mathbf{P}} | \mathbf{Q} = \langle \mathbf{Q} \rangle \cap \tilde{\mathbf{P}}, -I \notin \langle \mathbf{Q} \rangle, \mathbf{Q} = T_{cl}^\dagger Q T_{cl}\}. \quad (26)$$

Since $[Q, T_{cl}^\dagger Q T_{cl}] = 0$ for any $Q \in \mathbf{Q}$, $\mathbf{Q} \in \mathcal{S}_c(\mathbf{P})$, a naïve but useful simplification of $\mathcal{S}_c(\mathbf{P})$ is

$$\mathcal{S}_c(\mathbf{P}) = \mathcal{S}_c(\mathbf{P}'), \quad (27)$$

where $\mathbf{P}' = \{P \in \mathbf{P} | [P, T_{cl}^\dagger P T_{cl}] = 0\}$. Finally, the stabilizer ground state is given by

$$E_{\min} = \min_{c, \mathbf{Q} \in \mathcal{S}_c(\mathbf{P})} E_{\text{stab}}(H, \langle \mathbf{Q} \rangle). \quad (28)$$

The $\mathbf{Q} \in \mathcal{S}_c(\mathbf{P})$ minimizing Eq. (28) is referred as the **restricted maximally-commuting periodic Pauli subset**. In practice, we only need to determine \mathbf{Q} in one supercell, and \mathbf{Q} in other supercells must be the same due to $\mathbf{Q} = T_{cl}^\dagger Q T_{cl}$. For physically reasonable Hamiltonians, it might be enough to search for the minimum stabilizer ground state energy by checking the first a few c .

III. RESULTS

In this section, we first perform a few benchmarks on the exact 1D local algorithm, including (1) the computational cost in Sec. III A and (2) comparison with numerically optimized approximated stabilizer ground states in Sec. III B.

Furthermore, we demonstrate a few potential applications for stabilizer ground states and the corresponding algorithms on (1) generation of initial states for VQE problems for better performance in Sec. III C and (2) simple qualitative analysis of phase transitions in Sec. III D. Finally, in Sec. III E, we further develop an advanced ground state ansatz called extended stabilizer ground state to understand topological phase transitions in a 2D generalized toric code model [57].

All algorithms introduced in this work are implemented in both Python and C++ in https://github.com/SUSYUSTC/stabilizer_gs. The Python code is presented for concept illustration and readability, and the C++ code is used for optimal performance with a simple parallelization.

A. Computational cost of the exact 1D local algorithm

The scaling of the computation time for this exact 1D local algorithm only has a loose theoretical upper bound (Lemma 6 and Corollary 5) and lacks an exact analytical formula. Therefore, we implement the algorithm in C++ and numerically benchmark the computational time. All corresponding timings are collected on an 8-core i7-9700K Intel CPU.

We consider the following stochastic k -nearest Heisenberg model as the example Hamiltonian:

$$H = \sum_{i=1}^n \sum_{j=i+1}^{i+k-1} J_{ij}^{xx} S_i^x S_j^x + J_{ij}^{yy} S_i^y S_j^y + J_{ij}^{zz} S_i^z S_j^z \quad (29)$$

with each $J_{ij}^{xx}, J_{ij}^{yy}, J_{ij}^{zz} \sim \mathcal{N}(0, 1)$, i.e. all these coupling coefficients independently follow the normal distribution. We also consider the case of $J_{ij}^{zz} = 0, J_{ij}^{xx}, J_{ij}^{yy} \sim \mathcal{N}(0, 1)$ for comparisons. The two models are referred to as {XX,YY,ZZ} and {XX,YY}, respectively.

Following the procedure of the exact 1D local algorithm, all the possible values of $\{A_m\}$ with $m = 0, 2, \dots, n+1$ are generated sequentially by $A_m \rightarrow A_{m+1} \in F(A_m)$ with an initial state of $A_0 = A_0(\emptyset)$, where F is defined in Definition 9. In Figure 2(a), the computational costs of generating $\{A_{m+1}\}$ from $\{A_m\}$ are plotted as a function of site m for both the {XX,YY,ZZ} and {XX,YY} models with $n = 25$ and $k = 5$. Except for a few sites near the boundaries, the wall-clock time spent at each site is almost a constant for both models. This verifies that the computational cost of the 1D local algorithm scales as $O(n)$, as proved in Lemma 6. Due to the smaller number of Pauli terms in the Hamiltonian, the computational cost of the {XX,YY} model is systematically lower than the {XX,YY,ZZ} model.

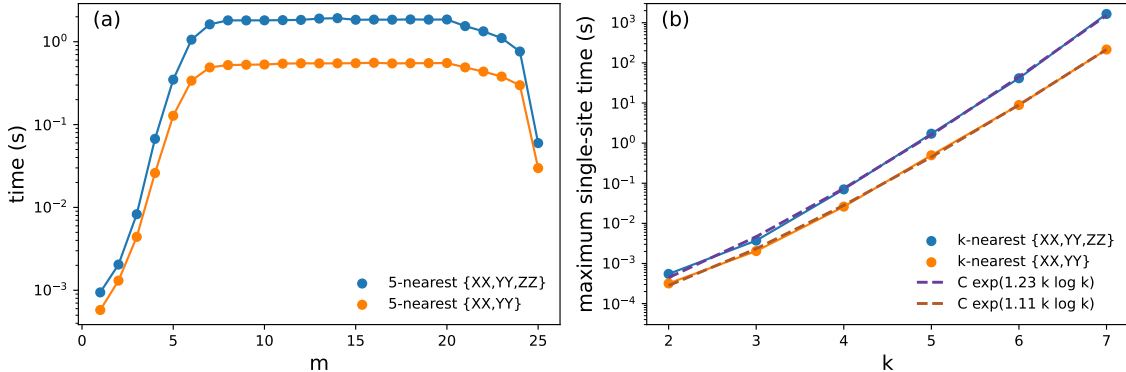


FIG. 2. Wall-clock time of the 1D local algorithm on the {XX,YY,ZZ} and {XX,YY} model (see the main text). (a) Computational time spent on each site m for the two models. (b) Maximum single-site computational time (solid lines) as a function of k for the two models, and fitted curves (dashed lines) with the form of $C \exp(C'k \log k)$.

After showing that the time spent at each site is a constant except for the sites near the boundaries, we further discuss the scaling of the maximum single-site running time as a function of the locality parameter k for different types of Hamiltonians. Figure 2(b) displays the maximum wall-clock time of a single site as a function of k for both models. We assume that the form of the scaling function is $C \exp(C'k \log k)$ according to Corollary 5. The numerical scaling functions are fitted independently for two models in Figure 2(b). The resulting fitted scaling curves have the parameters $C' = 1.23$ and $C' = 1.11$ for the {XX,YY,ZZ} and {XX,YY} models, respectively, and match the true

timing data well. This indicates that the computation time of different Hamiltonians within the same class scales similarly.

B. Comparison with numerical discrete optimizations of stabilizer ground states

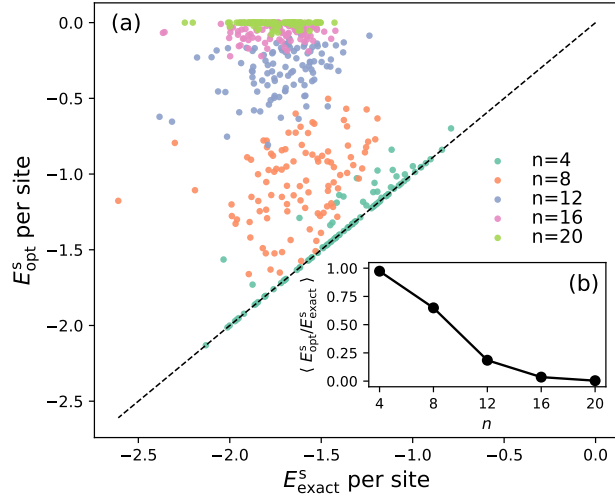


FIG. 3. Stabilizer ground state energies of the stochastic k -nearest Heisenberg model obtained by the exact 1D local algorithm (E_{exact}^s) and the numerical simulated annealing optimization algorithm (E_{opt}^s). (a) E_{exact}^s per site versus E_{opt}^s per site with $n = 4, 8, 12, 16, 20$ and $k = 4$. The black dashed line corresponds to $E_{\text{exact}}^s = E_{\text{opt}}^s$. (b) The mean relative energy error of stabilizer ground state energy captured by the numerical optimization algorithm ($\langle E_{\text{opt}}^s / E_{\text{exact}}^s \rangle$) versus n with locality $k = 4$.

We demonstrate that numerical optimizations of stabilizer ground states are not scalable and lead to unacceptable energy errors with an increasing number of qubits. The numerical optimization of stabilizer ground states can be performed by discrete optimizations of the Clifford circuits representing stabilizer states [58].

Here, we still use the stochastic k -nearest Heisenberg Hamiltonian in Eq. (29) (the $\{\text{XX}, \text{YY}, \text{ZZ}\}$ model) as an example. The Clifford ansatz employed here modifies the hardware-efficient Clifford ansatz in Ref. [58] by generalizing the single-qubit Clifford rotations to all single-qubit Clifford operations (24 unique choices in total) [59]. The simulated annealing algorithm is used in the discrete optimization with an exponential decay of temperature from 5 to 0.05 in 2500 steps. In each step of the simulated annealing, one of the single-qubit Clifford operations is randomly selected and replaced with one of the 24 operations, and the move is accepted with a probability of $\min(\exp(-\Delta E/T), 1)$, where ΔE is the energy difference.

Figure 3(a) compares the stabilizer ground state energies obtained from the exact 1D local algorithm (E_{exact}^s) and the numerical optimization algorithm (E_{opt}^s). For each n , 100 random Hamiltonians are tested. For every single test, the numerically optimized ground state energy is either equal to or higher than the exact stabilizer ground state energy. With increasing n , the success probability of the numerical optimization resulting in accurate stabilizer ground state energies decreases and E_{opt}^s approaches zero. This indicates that the numerical discrete optimization cannot correctly obtain the stabilizer ground state due to the exponential scaling of the number of stabilizer states and the number of possible Clifford circuits. Figure 3(b) displays the quantitative statistics of the performance degradation speed of numerical optimization by plotting the averaged relative stabilizer ground state energy $\langle E_{\text{opt}}^s / E_{\text{exact}}^s \rangle$ versus the number of sites n with $k = 4$. A rapid decay of the energy ratio is observed from 97.4% at $n = 4$ to 0.4% at $n = 20$. Therefore, the optimization method fails to bootstrap large-scale variational quantum algorithms via stabilizer initializations as claimed in Ref. [58] and the challenge is fully solved by our new algorithm at least in the 1D case.

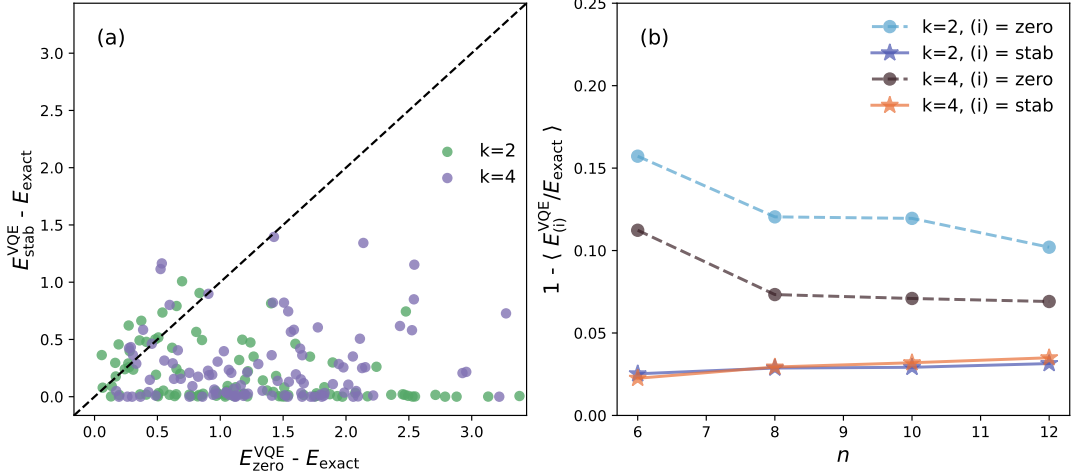


FIG. 4. Errors of optimized VQE energies computed using the stochastic k -nearest Heisenberg model. E_{exact} represents the exact ground state energy. $E_{\text{zero}}^{\text{VQE}}$ and $E_{\text{stab}}^{\text{VQE}}$ are the optimized VQE energies computed with stabilizer ground state initialization and the zero state initialization, respectively. (a) $E_{\text{stab}}^{\text{VQE}} - E_{\text{exact}}$ plots versus $E_{\text{zero}}^{\text{VQE}} - E_{\text{exact}}$ for $N = 100$ random Hamiltonians with $n = 6$ and $k = 2, 4$. (b) Mean relative errors of energies ($1 - (E_{(i)}^{\text{VQE}} / E_{\text{exact}})$) versus the number of sites n for the two initializations with $k = 2, 4$. The label (i)=zero indicates the zero state initialization, and (i)=stab indicates the stabilizer ground state initialization.

C. Initial state for VQE problems

Stabilizer states have been recently used as initial states [58, 60] for VQE problems to mitigate the notorious barren plateau issue [61–63]. The stabilizer initial states can be prepared on quantum circuits by efficient decomposition to up to $O(n^2 / \log n)$ single-qubit and double-qubit Clifford gates [25]. The effective VQE ansatz is

$$|\psi(\boldsymbol{\theta})\rangle = U(\boldsymbol{\theta})|\psi_{\text{stab}}\rangle = U(\boldsymbol{\theta})U_C|0\rangle^{\otimes n}, \quad (30)$$

where the stabilizer initial state $|\psi_{\text{stab}}\rangle$ is decomposed to $U_C|0\rangle^{\otimes n}$. Another approach is to employ the quantum state ansatz as follows:

$$|\psi(\boldsymbol{\theta})\rangle = U_C U(\boldsymbol{\theta})|0\rangle^{\otimes n}. \quad (31)$$

The advantage of the latter approach is that one can equivalently transform the Hamiltonian by $H \rightarrow H' = U_C^\dagger H U_C$ classically, and thus only the $U(\boldsymbol{\theta})$ part needs to be performed on the quantum circuit [47, 48, 64]. However, its disadvantage is that it might break the locality of the Hamiltonian and cause additional costs on the hardware that cannot support nonlocal operations [65, 66]. Therefore, we adopt the former strategy in Eq. (30) for the following benchmark.

The $\{\text{XX}, \text{YY}, \text{ZZ}\}$ model in Eq. (29) still serves as the example Hamiltonian, and the variational Hamiltonian ansatz [67] is used as the example VQE circuit for ground state optimization. By rewriting the Hamiltonian as $H = \sum_P w_P P$ with $P = S_i^x S_j^x, S_i^y S_j^y, S_i^z S_j^z$, the corresponding quantum circuit ansatz is as follows:

$$|\psi(\boldsymbol{\theta})\rangle = \prod_P e^{i\theta_P P} |\psi_{\text{init}}\rangle. \quad (32)$$

We compare two choices of the initial state $|\psi_{\text{init}}\rangle$, including the $|0\rangle^{\otimes n}$ state (referred to as zero state) and the stabilizer ground state obtained by the exact 1D local algorithm. The quantum circuit simulations are conducted via the *TensorCircuit* software [68]. The optimization of parameters $\boldsymbol{\theta}$ is performed by the default L-BFGS-B [69] optimizer in *SciPy* [70] with zero initial values.

Figure 4(a) displays the distributions of optimized energy errors obtained from the two initialization strategies tested on 100 random Hamiltonians with $n = 6$. Stabilizer state initializations result in lower VQE errors compared with those via the zero state in 82% and 92% of the 100 tests for $k = 2$ and $k = 4$, respectively. There are few points in the region of $E_{\text{zero}}^{\text{VQE}} < E_{\text{stab}}^{\text{VQE}}$, which is attributed to the fact that an initialization state with a lower energy does not guarantee a lower final energy after VQE optimizations. Figure 4(b) also shows the mean relative errors of energies

$1 - \langle E_{(i)}^{\text{VQE}} / E_{\text{exact}} \rangle$ for increasing n and $k = 2, 4$, where (i) represents each initialization strategy. Initializations via stabilizer ground states are observed to systematically provide better energy estimations for both $k = 2$ and $k = 4$.

D. Qualitative analysis of phase transitions

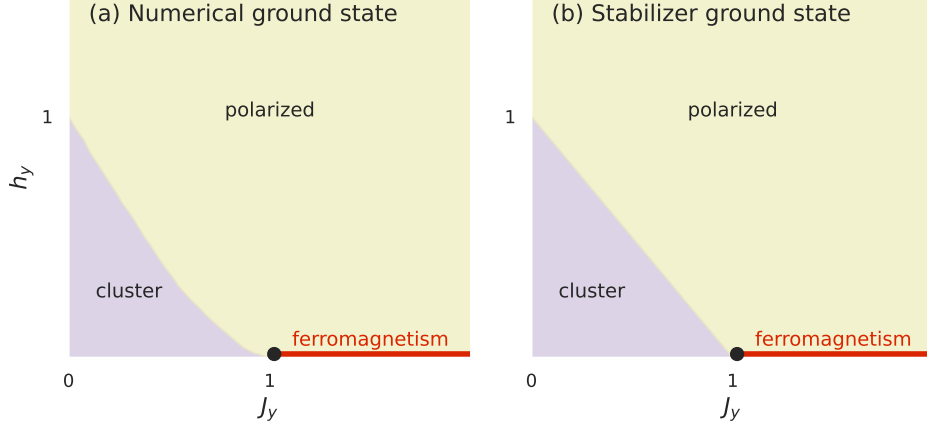


FIG. 5. Ground state phase diagram of the Hamiltonian in Eq. (33) obtained by (a) numerical DMRG calculations in Ref. [71] and (b) stabilizer ground state calculations via the exact 1D periodic local algorithm. There are three phases, including the cluster phase, the polarized phase and the ferromagnetism phase, for both cases.

Similar to the mean-field states, stabilizer ground states can also qualitatively capture the phases and phase transitions in many interesting systems. Specifically, stabilizer ground states are good at capturing topological phases with long-range entanglements. This capability is demonstrated using an infinite 1D generalized cluster model [71] as an example, whose Hamiltonian is

$$H = \sum_{n=-\infty}^{\infty} -X_{n-1}Z_nX_{n+1} - J_yY_nY_{n+1} + h_yY_n. \quad (33)$$

This model is equivalent to the free fermion model at $h_y = 0$, while it is not dual to any free fermion model at $h_y \neq 0$ due to the lack of Z_2 symmetry. This Hamiltonian has been studied by numerical density matrix renormalization group (DMRG) calculations in Ref. [71], and the corresponding phase diagram is replotted in Figure 5(a). Three phases are observed in this phase diagram, including the symmetry-protected topological phase at small but positive J_y and h_y , the polarized phase at $J_y \rightarrow \infty$, $h_y \rightarrow \infty$, and the ferromagnetic phase at $h_y = 0, J_y > 1$.

We apply the exact 1D periodic local algorithm to the Hamiltonian to obtain the stabilizer ground states of this model using different parameters (J_y, h_y) . Calculations are performed with candidate supercell sizes $c \leq 6$, and the minimum energy is selected as the stabilizer ground state energy. All possible types of distinct stabilizer ground states are listed in Table I, and the corresponding phase diagram is plotted in Figure 5(b). When comparing Figure 5 (a) and (b), the stabilizer ground state phase diagram matches the numerical ground state phase diagram well except for the shape of the boundary between the cluster phase and the polarized phase. The boundary predicted by stabilizer ground states is a straight line, while the numerical boundary is slightly curved. These agreements indicate that stabilizer ground states are useful to qualitatively understand of phase transitions in quantum many-body systems and provide a new perspective compared to conventional mean-field approaches. The stabilizer ground state at the tricritical point $J_y = 1, h_y = 0$ is observed to have two new degenerate stabilizer ground states besides the stabilizer ground states in other phases. These two new stabilizer ground states have stabilizers $\{X_{3n-1}Z_{3n}X_{3n+1}, Y_{3n-1}Y_{3n}, Y_{3n}Y_{3n+1}\}$ and $\{X_{3n-1}Z_{3n}X_{3n+1}, X_{3n}Z_{3n+1}X_{3n+2}, Y_{3n}Y_{3n+1}\}$, respectively.

E. Extended stabilizer ground states

Stabilizer ground states can be used as a platform to develop advanced numerical methods or quantum state ansatz. As an illustration, we introduce the extended stabilizer ground state and demonstrate its capability of characterizing

TABLE I. Stabilizer ground states of the Hamiltonian in Eq. (33) in different phases. Note that the conditions of (J_y, h_y) do not strictly contradict each other, which indicates degeneracies of stabilizer ground states in the overlap regions (borders between phases or the tricritical point).

Stabilizers	(J_y, h_y)	Phase
$\{X_{n-1}Z_nX_{n+1}\}$	$J_y + h_y \leq 1$	Cluster
$\{-Y_n\}$	$J_y + h_y \geq 1, h_y > 0$	Polarized
$\{Y_nY_{n+1}\}$	$J_y \geq 1, h_y = 0$	Ferromagnetism
$\{X_{3n-1}Z_{3n}X_{3n+1}, Y_{3n-1}Y_{3n}, Y_{3n}Y_{3n+1}\}$	$J_y = 1, h_y = 0$	Tricritical point
$\{X_{3n-1}Z_{3n}X_{3n+1}, X_{3n}Z_{3n+1}X_{3n+2}, Y_{3n}Y_{3n+1}\}$	$J_y = 1, h_y = 0$	Tricritical point

phase transitions of a 2D generalized toric code model. We first introduce a quantum state ansatz expressed as applying single-qubit rotations on some stabilizer states, i.e.

$$|\psi\rangle = U(\{\theta_j\})|\psi_{\text{stab}}\rangle = \prod_j e^{i\theta_j \cdot \mathbf{S}_j} |\psi_{\text{stab}}\rangle, \quad (34)$$

where \mathbf{S}_j is the vector spin operator on the j th qubit. We then define the extended stabilizer ground state by the state $|\psi\rangle$ with the lowest energy among all possible combinations of $\{\theta_j\}$ and $|\psi_{\text{stab}}\rangle$. Instead of directly finding the value of $\{\theta_j\}$ and $|\psi_{\text{stab}}\rangle$ that minimizes the energy, we can effectively transform the Hamiltonian by

$$H \rightarrow H'(\{\theta_j\}) = U^\dagger(\{\theta_j\}) H U(\{\theta_j\}). \quad (35)$$

The stabilizer ground state of the Hamiltonian $H'(\{\theta_j\})$ is thus a function of $\{\theta_j\}$. Since local Hamiltonians after single-site rotations remain local with the same localities k , such an extended stabilizer ground state formalism increases the expressive power without significantly complicating the problem, especially when each Pauli operator only nontrivially acts on a limited number of sites.

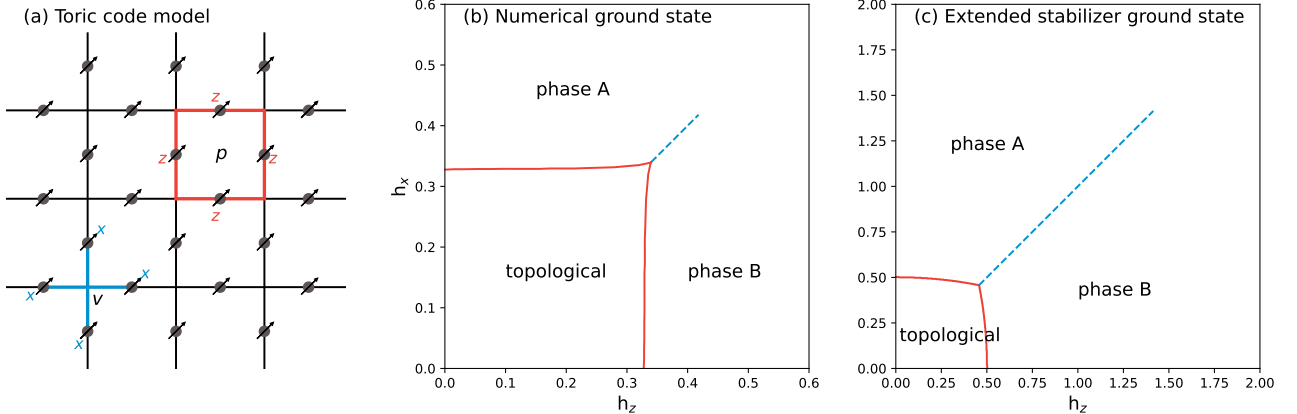


FIG. 6. Geometry and phase diagrams of the 2D generalized toric code. (a) Geometry of the 2D generalized toric code model in Eq. (36). (b) Numerical ground state phase diagram obtained by continuous-time Monte Carlo calculations in Ref. [72]. (c) Extended stabilizer ground state phase diagram. For both (b) and (c), three phases are found, including the topological phase, phase A, and phase B. The first-order transition line (dashed blue line) at $h_x = h_z$ begins at $h_x = h_z = 0.34$ and ends at $h_x = h_z = 0.418$ in (b), while it begins at $h_x = h_z = 0.46$ and ends at $h_x = h_z = 1.414$ in (c)

As a demonstration, we consider a 2D generalized toric code model with external magnetic fields. The Hamiltonian is

$$H = - \left(\sum_v A_v + \sum_p B_p \right) - h_x \sum_j X_j - h_z \sum_j Z_j, \quad (36)$$

which is defined on a torus, where $A_v = \prod_{j \in v} X_j$ and $B_p = \prod_{j \in p} Z_j$ represent the product of spin operators on bonds incident to the vertex v and surrounding plaquette p , respectively. The geometry of the vertices and plaquettes is shown in Figure 6(a). This Hamiltonian is studied by continuous-time Monte Carlo simulation in Ref. [72] and the

phase diagram is reproduced in Figure 6(b). At $h_x \rightarrow \infty$ with fixed h_z or $h_z \rightarrow \infty$ with fixed h_x , each spin is polarized in the x or z direction, and gives the phase A or B, respectively. A phase transition happens between the phase A and B at the first-order transition line $h_x = h_z$, which begins at $h_x = h_z = 0.34$ and ends at $h_x = h_z = 0.418$. In the limit of $h_x \rightarrow \infty$ and $h_z \rightarrow \infty$, the polarization of the system varies continuously between phases A and B, thus no phase transition occurs.

Now we consider the extended stabilizer ground state of this Hamiltonian. Since the Hamiltonian only contains X and Z, the single-qubit rotations can be restricted to the form of $U(\{\theta_j\}) = \prod_j e^{\frac{1}{2}i\theta_j Y_j}$. As stated previously, we need to transform the Hamiltonian in Eq. (36) by $U(\{\theta_j\})$ and then determine the stabilizer ground state. As discussed in Sec. IID, the stabilizer ground state of a periodic local Hamiltonian should be periodic over supercells with some size c . For simplification, the stabilizer ground state is assumed to have period 1. We set $\theta_j = \alpha$ and $\theta_j = \beta$ for sites j on vertical bonds and horizontal bonds, respectively, and thus the total rotation operator can be written as $U(\alpha, \beta)$.

With fixed supercell size $c = 1$, the stabilizer ground state of the rotated Hamiltonian $U(\alpha, \beta)^\dagger H U(\alpha, \beta)$ can be found via Eq. (28) for each set of rotation angles α, β . The corresponding stabilizer ground state energy per site is written as $E(h_x, h_z, \alpha, \beta)$. The extended stabilizer ground state energy per site is then given by $E(h_x, h_z) = \min_{\alpha, \beta} E(h_x, h_z, \alpha, \beta)$. In the following analysis, we apply the simplification process in Eq. (27) for convenience, which allows us to exclude Pauli terms like $P = X_l Z_r X_u Z_d$, where the subscripts l, r, u, d stand for the left, right, up, and down site of either a vertex or a plaquette. The valid Pauli terms of the rotated Hamiltonians include (1) X and Z on each site; and (2) $X_l X_r X_u X_d, X_l X_r Z_u Z_d, Z_l Z_r X_u X_d$, and $Z_l Z_r Z_u Z_d$ on each vertex or plaquette.

The resulting extended stabilizer ground state phase diagram is plotted in Figure 6(c) and it matches the exact phase diagram qualitatively. In the topologically ordered phase, the stabilizers are the set of all $X_l X_r X_u X_d, X_l X_r Z_u Z_d, Z_l Z_r X_u X_d, Z_l Z_r Z_u Z_d$ on all vertices and plaquettes. We find that the corresponding $E(h_x, h_z, \alpha, \beta)$ is a constant with respect to α and β , attributed to the fact that $U(\alpha, \beta)$ is a symmetry operation of this stabilizer state. In phase A and B, the stabilizers are simply X on each site and $X_l X_r X_u X_d$ on each vertex and plaquette, which corresponds to the product of single-site polarized states in the picture of the unrotated Hamiltonian. We consider the first-order transition line at $h_x = h_z$, in which case the extended stabilizer ground state is always found at $\alpha = \beta$. The corresponding per-site energy function $E(h, \alpha) = E(h_x = h, h_z = h, \alpha, \beta = \alpha)$ is given by

$$E(h, \alpha) = -\frac{1}{2}(\cos^4 \alpha + \sin^4 \alpha) - h(\cos \alpha + \sin \alpha), \quad (37)$$

which is symmetric under $\alpha \rightarrow \frac{\pi}{2} - \alpha$. No phase transition happens for large h since only one minimum $\alpha = \frac{\pi}{4}$, while two minimums can be found for small h . This is a signal of the end of the first-order transition. It is located at

$$\frac{\partial^2 E(h, \alpha)}{\partial \alpha^2} \Big|_{\alpha=\frac{\pi}{4}} = \sqrt{2}h - 2 = 0, \quad (38)$$

which gives $h = \sqrt{2}$. Furthermore, at $h < h_c \approx 0.46$, $E(h, \alpha)$ is higher than the energy of the topologically ordered state for all α . Thus, we claim that the corresponding first-order transition line begins at $h_x = h_z \approx 0.46$ and ends at $h_x = h_z = \sqrt{2} \approx 1.414$. Although the exact transition values are different, the qualitative picture obtained by the extended stabilizer ground state is consistent with the ground truth.

IV. CONCLUSIONS AND OUTLOOK

In this work, we introduce the concept of stabilizer ground states as a versatile toolkit to qualitatively analyze quantum systems, improve quantum algorithms, and develop advanced ground state ansatzes. For general Hamiltonians, we establish the equivalence between the stabilizer ground state and the restricted maximally-commuting Pauli subset. For 1D local Hamiltonians, we additionally developed an exact and efficient algorithm that ensures a linear computational scaling with the system size to obtain the stabilizer ground state. We further extend the formalism for general Hamiltonians and the linear-scaled algorithm for 1D local Hamiltonians to infinite periodic systems. By benchmarking on example Hamiltonians, we verified the computational scaling of the exact 1D local algorithm and demonstrated the substantial performance gain over the traditional discrete optimization strategies. We also illustrate that stabilizer ground states are promising tools for various applications, including qualitative analysis of phase transitions, generating better heuristics for VQE problems, and developing more expressive ground state ansatzes.

Looking forward, future studies can fruitfully branch into three major directions. The first avenue is to delve into algorithms for stabilizer ground states of Hamiltonians with more sophisticated structures. A promising example would be generalizing the 1D local algorithm to other quasi-1D structures, such as structures with closed loops and tree-like lattice structures. For local Hamiltonians in higher dimensions, finding the exact stabilizer ground state can be proved as NP-hard, evidenced by the NP-hardness of one of its simplified cases, i.e., the ground state problem of 2D

classical spin models with random magnetic fields [73, 74]. Nonetheless, approximate or heuristic algorithms [75, 76] for stabilizer ground states may still be practically useful for higher dimensional systems. The second avenue extends the concept of the stabilizer ground states to other physically interested properties, like excited states and thermal state sampling. These extensions are plausible as the automaton structure of the 1D algorithm shares similarities with an ensemble of quantum states. The third avenue involves the exploration of more downstream applications for stabilizer ground states. Possible candidates include developing advanced numerical methods via perturbation theories [45] or low-rank (or low-energy) stabilizer decomposition [43].

ACKNOWLEDGEMENT

J.S. gratefully acknowledges the support from Hongyan Scholarship.

V. APPENDIX

A. Proof of Theorem 1

Proof. Let $\mathbf{S} = \langle \mathbf{Q} \rangle$, $\mathbf{Q} \in \mathcal{S}(\mathbf{P})$ be one of the stabilizer group such that $E_{\text{stab}}(H, \mathbf{S}) = E_{\min}$, and $|\psi\rangle$ is any stabilizer state stabilized by \mathbf{S} . Let $\mathbf{S}_\psi = \langle \text{Stab}(|\psi\rangle) \cap \tilde{\mathbf{P}} \rangle$, obviously we have $\mathbf{S} \subseteq \mathbf{S}_\psi$. Let $\mathbf{S}_\psi = \langle \mathbf{S}, P_1, P_2, \dots, P_k \rangle$ where each $P_i \in \tilde{\mathbf{P}}$, $1 \leq i \leq k$. We consider the sequence $\mathbf{S}_i = \langle \mathbf{S}, P_1, P_2, \dots, P_i \rangle$ with $i = 0, 1, \dots, k$. Clearly we have $\mathbf{S}_i = \langle \mathbf{Q}_i \rangle$, $\mathbf{Q}_i = \mathbf{S}_i \cap \tilde{\mathbf{P}} \in \mathcal{S}(\mathbf{P})$ for each \mathbf{S}_i .

First we prove $E_{\text{stab}}(H, \mathbf{S}_i) = E_{\min}$ for each \mathbf{S}_i . Obviously it is true for $i = 0$. Given it is true for \mathbf{S}_i , we then consider $\mathbf{S}_{i+1} = \langle \mathbf{S}_i, P_{i+1} \rangle$. If $P_{i+1} \in \mathbf{S}_i$, then $\mathbf{S}_{i+1} = \mathbf{S}_i$ so $E_{\text{stab}}(H, \mathbf{S}_{i+1}) = E_{\min}$. Otherwise we consider $E_i = E_{\text{stab}}(H, \mathbf{S}_i)$, $E_+ = E_{\text{stab}}(H, \langle \mathbf{S}_i, P_{i+1} \rangle)$ and $E_- = E_{\text{stab}}(H, \langle \mathbf{S}_i, -P_{i+1} \rangle)$. For each $P \in \mathbf{P}$, it falls into one of the following situations: (1) $P \in \pm \mathbf{S}_i$ so it contributes equally to E_i , E_+ and E_- , (2) $P \notin \pm \mathbf{S}_i$ but $P \in \pm \langle \mathbf{S}_i, P_{i+1} \rangle$ so it contributes no energy to E_i and opposite energy to E_+ and E_- , (3) $P \notin \pm \langle \mathbf{S}_i, P_{i+1} \rangle$ so it contributes no energy to E_i , E_+ and E_- . Thus we have $2E_i = E_+ + E_-$. However E_i is already the minimum of $E_{\text{stab}}(H, \mathbf{S})$ for $\mathbf{S} \in \mathcal{S}(\mathbf{P})$, thus $E_+ = E_- = E_i = E_{\min}$, i.e. $E_{\text{stab}}(H, \mathbf{S}_{i+1}) = E_{\min}$. Now we can conclude that $E_{\text{stab}}(H, \mathbf{S}_i) = E_{\min}$ for each \mathbf{S}_i , which implies $E_{\text{stab}}(H, \mathbf{S}_\psi) = E_{\min}$.

Next, we prove $|\psi\rangle$ is a (degenerate) stabilizer ground state. According to Corollary 1, we have $\langle \psi | H | \psi \rangle = E_{\text{stab}}(H, \mathbf{S}_\psi) = E_{\min}$. If there exists stabilizer state $|\psi'\rangle$ such that $\langle \psi' | H | \psi' \rangle < \langle \psi | H | \psi \rangle = E_{\min}$, we should have $E_{\text{stab}}(H, \langle \text{Stab}(|\psi'\rangle) \cap \tilde{\mathbf{P}} \rangle) = \langle \psi' | H | \psi' \rangle < E_{\min}$, which conflicts with the definition of E_{\min} . Thus we conclude that $|\psi\rangle$ is a (degenerate) stabilizer ground state. \square

B. Validity of \mathbf{Q}_m for A_m constructed by F

We prove the validity of \mathbf{Q}_m by showing that, as long as $\mathbf{Q}_{m'}$ is valid for any $m' \leq m$, then \mathbf{Q}_{m+1} is also valid.

Lemma 7. Let $\{A_{i=0}^{m+1}\}$ be a path such that $A_0 = A_0(\emptyset)$ and $A_{i+1} \in F(A_i)$, $0 \leq i \leq m$. It naturally defines $\mathbf{Q}_i = \mathbf{S}_{\text{right}}^i \cap \tilde{\mathbf{P}}_i$ for $i \leq m+1$. If the statement that (1) \mathbf{Q}_i is valid to add to $\mathbf{Q}_{<i}$, and (2) $\langle \mathbf{Q}_{<i}, \mathbf{S}_{\text{right}}^i \rangle \cap \tilde{\mathbf{P}}_{<i} = \mathbf{Q}_{<i}$ is true for each $i \leq m$, then it is also true for $i = m+1$.

Proof. Since each \mathbf{Q}_i is valid, we have $\mathbf{S}_{\text{proj}}^i = \mathbf{S}_{\text{proj}}^i(\mathbf{Q}_{<i})$, $\tilde{\mathbf{P}}_{\text{invalid}}^i = \tilde{\mathbf{P}}_{\text{invalid}}^i(\mathbf{Q}_{<i})$ for $i \leq m+1$. We then prove two intermediate conclusions:

First we prove $[\mathbf{Q}_{<m+1}, \mathbf{S}_{\text{right}}^{m+1}] = 0$ from rule 2(b). In fact we have $[\mathbf{Q}_{<m+1}, \tilde{\mathbf{P}}_{\geq m+1} - \tilde{\mathbf{P}}_{\text{invalid}}^{m+1}] = 0$ from $\tilde{\mathbf{P}}_{\text{invalid}}^{m+1} = \tilde{\mathbf{P}}_{\text{invalid}}^{m+1}(\mathbf{Q}_{<m+1})$. Since the commutation/anticommutation relations between Paulis P and Q only depends on their values at shared sites, we must have $[\mathbf{Q}_{<m+1}, \mathbb{T}_{m-k+2, m+1}(\tilde{\mathbf{P}}_{\geq m+1} - \tilde{\mathbf{P}}_{\text{invalid}}^{m+1})] = 0$. Thus $[\mathbf{Q}_{<m+1}, \mathbf{S}_{\text{right}}^{m+1}] = 0$.

Then according to rule 2(c) in Definition 9 we have

$$\begin{aligned}
\mathbf{Q}_m &= \langle \mathbf{S}_{\text{proj}}^m, \mathbf{S}_{\text{right}}^m \rangle \cap \tilde{\mathbf{P}}_m \\
&= \langle \mathbb{P}_{m-k+1,m}(\langle \mathbf{Q}_{<m} \rangle), \mathbf{S}_{\text{right}}^m \rangle \cap \tilde{\mathbf{P}}_m \\
&= \mathbb{P}_{m-k+1,m}(\langle \mathbf{Q}_{<m}, \mathbf{S}_{\text{right}}^m \rangle) \cap \tilde{\mathbf{P}}_m \\
&= \langle \mathbf{Q}_{<m}, \mathbf{S}_{\text{right}}^m \rangle \cap \tilde{\mathbf{P}}_m,
\end{aligned} \tag{39}$$

where we used $\mathbf{S}_{\text{right}}^m \subseteq \mathcal{P}_{m-k+1,m}$ in the second line.

Combining the above two intermediate conclusions, we finally have

$$\begin{aligned}
\langle \mathbf{Q}_{<m+1}, \mathbf{S}_{\text{right}}^{m+1} \rangle \cap \tilde{\mathbf{P}}_{<m+1} &= \langle \mathbf{Q}_{<m}, \mathbf{Q}_m, \mathbf{S}_{\text{right}}^{m+1} \rangle \cap \tilde{\mathbf{P}}_{<m+1} \\
&= \langle \mathbf{Q}_{<m}, \mathbb{P}_{m-k+1,m}(\langle \mathbf{S}_{\text{right}}^{m+1}, \mathbf{Q}_m \rangle) \rangle \cap \tilde{\mathbf{P}}_{<m+1} \\
&= \langle \mathbf{Q}_{<m}, \mathbf{S}_{\text{right}}^m \rangle \cap \tilde{\mathbf{P}}_{<m+1} \\
&= (\langle \mathbf{Q}_{<m}, \mathbf{S}_{\text{right}}^m \rangle \cap \tilde{\mathbf{P}}_{<m}) \cup (\langle \mathbf{Q}_{<m}, \mathbf{S}_{\text{right}}^m \rangle \cap \tilde{\mathbf{P}}_m) \\
&= \mathbf{Q}_{<m} \cup \mathbf{Q}_m \\
&= \mathbf{Q}_{<m+1},
\end{aligned} \tag{40}$$

which finishes the part (2) of the statement for $i = m+1$. Rule 2(d) is used in the third line, and Eq. (39) is used in the fifth line. As a consequence, we also have $\langle \mathbf{Q}_{<m+1}, \mathbf{S}_{\text{right}}^{m+1} \cap \tilde{\mathbf{P}}_{m+1} \rangle \cap \tilde{\mathbf{P}}_{m+1} = \mathbf{Q}_{<m+1}$, i.e. $\langle \mathbf{Q}_{<m+1}, \mathbf{Q}_{m+1} \rangle \cap \tilde{\mathbf{P}}_{m+1} = \mathbf{Q}_{<m+1}$, which is exactly the last condition of Corollary 4 for qubit $m+1$. Combined with rule 2(a), we can conclude that \mathbf{Q}_{m+1} is valid to add to $\mathbf{Q}_{<m+1}$, which finishes the part (1) of the statement. \square

C. One-to-one correspondence between $\{A_{i=0}^{n+1}\}$ generated by F and $\mathbf{Q} \in \mathcal{S}(\mathbf{P})$

In order to prove such one-to-one correspondence, we need to prove (1) each path $\{A_{i=0}^{n+1}\}$ generated from $A_0 = A_0(\emptyset)$ and $A_{m+1} \in F(A_m)$ is exactly some $\{A_{i=0}^{n+1}(\mathbf{Q} \in \mathcal{S}(\mathbf{P}))\}$, and (2) each $\{A_{i=0}^{n+1}(\mathbf{Q} \in \mathcal{S}(\mathbf{P}))\}$ is a path generated from $A_0 = A_0(\emptyset)$ and $A_{m+1} \in F(A_m)$.

We first prove the former one:

Lemma 8. *For any path $\{A_{m=0}^{n+1}\}$ such that $A_0 = A_0(\emptyset)$ and $A_{m+1} \in F(A_m)$, $0 \leq m < n+1$, there exists $\mathbf{Q} \in \mathcal{S}(\mathbf{P})$ such that $A_m = A_m(\mathbf{Q})$ for each m .*

Proof. Let $\mathbf{Q} = \cup_{m=1}^n \mathbf{Q}_m$ with $\mathbf{Q}_m = \mathbf{S}_{\text{right}}^m \cap \tilde{\mathbf{P}}_m$. According to Lemma 7, each \mathbf{Q}_m is valid to add to $\langle \mathbf{Q}_{<m} \rangle$ since the statement at $i = 0$ is trivially satisfied. Thus we automatically have $\mathbf{S}_{\text{proj}}^m = \mathbf{S}_{\text{proj}}^m(\mathbf{Q}_{<m})$ and $\tilde{\mathbf{P}}_{\text{invalid}}^m = \tilde{\mathbf{P}}_{\text{invalid}}^m(\mathbf{Q}_{<m})$ for each m . We then prove $\mathbf{S}_{\text{right}}^m = \mathbf{S}_{\text{right}}^m(\mathbf{Q}_{\geq m})$. We begin with $m = n+1$, where we have $\mathbf{S}_{\text{right}}^n \in \mathcal{S}(\emptyset)$ according to rule 2(b) in Definition 9, thus $\mathbf{S}_{\text{right}}^{n+1} = \langle \emptyset \rangle$ and $\mathbf{S}_{\text{right}}^m = \mathbf{S}_{\text{right}}^m(\mathbf{Q}_{\geq m})$ holds at $m = n+1$. If it holds for m , according to rule 2(d) in Definition 9, we have

$$\begin{aligned}
\mathbf{S}_{\text{right}}^{m-1} &= \langle \mathbb{P}_{m-k,m-1}(\mathbf{S}_{\text{right}}^m), \mathbf{Q}_{m-1} \rangle \\
&= \langle \mathbb{P}_{m-k,m-1}(\mathbf{Q}_{\geq m}), \mathbf{Q}_{m-1} \rangle \\
&= \mathbb{P}_{m-k,m-1}(\mathbf{Q}_{\geq m-1}) \\
&= \mathbf{S}_{\text{right}}^{m-1}(\mathbf{Q}_{\geq m-1}).
\end{aligned}$$

Thus $\mathbf{S}_{\text{right}}^m = \mathbf{S}_{\text{right}}^m(\mathbf{Q}_{\geq m})$ holds for each m . Finally we conclude that $A_m = A_m(\mathbf{Q})$ for each m . \square

To prove the latter one, it suffices to prove:

Lemma 9. *For any $\mathbf{Q} \in \mathcal{S}(\mathbf{P})$, $A_{m+1}(\mathbf{Q}) \in F(A_m(\mathbf{Q}))$ for each m .*

Proof. We only need to show that the rules in Definition 9 are satisfied for each $A_m = A_m(\mathbf{Q})$ and $A_{m+1} = A_{m+1}(\mathbf{Q})$. We check them one by one.

1. Rule 2(a) is obvious according to Lemma 5.

2. For rule 2(b) we have

$$\begin{aligned}
\mathbf{S}_{\text{right}}^{m+1}(\mathbf{Q}) &= \mathbb{P}_{m-k+2, m+1}(\langle \mathbf{Q}_{\geq m+1} \rangle) \\
&\subseteq \mathbb{P}_{m-k+2, m+1}(\langle \tilde{\mathbf{P}}_{\geq m+1} - \tilde{\mathbf{P}}_{\text{invalid}}^{m+1}(\mathbf{Q}) \rangle) \\
&\in \mathcal{S}(\mathbb{T}_{m-k+2, m+1}(\tilde{\mathbf{P}}_{\geq m+1} - \tilde{\mathbf{P}}_{\text{invalid}}^{m+1}(\mathbf{Q}))). \tag{41}
\end{aligned}$$

3. For rule 2(c), with

$$\begin{aligned}
\mathbf{Q}_{m+1} &= \mathbf{S}_{\text{right}}^{m+1}(\mathbf{Q}_{\geq m+1}) \cap \tilde{\mathbf{P}}_{m+1} \\
&\subseteq \langle \mathbf{S}_{\text{proj}}^{m+1}(\mathbf{Q}_{< m+1}), \mathbf{S}_{\text{right}}^{m+1}(\mathbf{Q}_{\geq m+1}) \rangle \cap \tilde{\mathbf{P}}_{m+1}, \tag{42}
\end{aligned}$$

and

$$\langle \mathbf{S}_{\text{proj}}^{m+1}(\mathbf{Q}_{< m+1}), \mathbf{S}_{\text{right}}^{m+1}(\mathbf{Q}_{\geq m+1}) \rangle \subseteq \langle \mathbf{Q} \rangle, \tag{43}$$

we have

$$\langle \mathbf{S}_{\text{proj}}^{m+1}(\mathbf{Q}_{< m+1}), \mathbf{S}_{\text{right}}^{m+1}(\mathbf{Q}_{\geq m+1}) \rangle \cap \tilde{\mathbf{P}}_{m+1} = \mathbf{Q}_{m+1}. \tag{44}$$

4. For rule 2(d) we have

$$\begin{aligned}
\mathbf{S}_{\text{right}}^m(\mathbf{Q}) &= \mathbb{P}_{m-k+1, m}(\langle \mathbf{Q}_{\geq m} \rangle) \\
&= \langle \mathbb{P}_{m-k+1, m}(\mathbf{Q}_{\geq m+1}), \mathbf{Q}_m \rangle \\
&= \langle \mathbb{P}_{m-k+1, m}(\mathbf{S}_{\text{right}}^m(\mathbf{Q})), \mathbf{Q}_m \rangle. \tag{45}
\end{aligned}$$

□

Combining the Lemma 8 and Lemma 9, we have proved the one-to-one correspondence between $\{A_{i=0}^{n+1}\}$ generated by F and $\mathbf{Q} \in \mathcal{S}(\mathbf{P})$.

D. Proof of Lemma 6

Proof. According to Lemma 7, for each (partial) path $\{A_{i=0}^m\}$, let $\mathbf{Q}_{< m} = \cup_{i < m} \mathbf{Q}_i = \cup_{i < m} \mathbf{S}_{\text{right}}^i \cap \tilde{\mathbf{P}}_i$, we always have $\mathbf{Q}_{< m} \in \mathcal{S}(\mathbf{P}_{< m})$, $\mathbf{S}_{\text{proj}}^m = \mathbf{S}_{\text{proj}}^m(\mathbf{Q}_{< m})$ and $\tilde{\mathbf{P}}_{\text{invalid}}^m = \tilde{\mathbf{P}}_{\text{invalid}}^m(\mathbf{Q}_{< m})$, even if some elements in $\{A_{i=0}^m\}$ are “divergent branches”. In the following, we give the upper bound of the number of pairs $(\mathbf{S}_{\text{proj}}^m, \tilde{\mathbf{P}}_{\text{invalid}}^m)$ and the number of $\mathbf{S}_{\text{right}}^m$ separately.

First, we prove that the pair $(\mathbf{S}_{\text{proj}}^m, \tilde{\mathbf{P}}_{\text{invalid}}^m)$ can be determined from

$$\mathbf{S}' = \mathbb{P}_{m-2k+2, m-1}(\langle \mathbf{Q}_{< m} \rangle). \tag{46}$$

For $\mathbf{S}_{\text{proj}}^m$ we have

$$\begin{aligned}
\mathbf{S}_{\text{proj}}^m &= \mathbb{P}_{m-k+1, m-1}(\langle \mathbf{Q}_{< m} \rangle) \\
&= \mathbb{P}_{m-k+1, m-1}(\mathbf{S}'). \tag{47}
\end{aligned}$$

For $\tilde{\mathbf{P}}_{\text{invalid}}^m$, since $P \in \tilde{\mathbf{P}}_{\geq m}$ has $q_P^{\text{begin}} \geq m - k + 1$, any $Q \in \mathbf{Q}_{< m}$ with $\{P, Q\} = 0$ must have $q_P^{\text{last}} \geq m - k + 1$ and thus $q_P^{\text{begin}} \geq m - 2k + 2$, so we have $Q \in \mathbf{S}'$. Thus

$$\begin{aligned}
\tilde{\mathbf{P}}_{\text{invalid}}^m &= \{P \in \tilde{\mathbf{P}}_{\geq m} \mid [P, \mathbf{Q}_{< m}] \neq 0\} \\
&= \{P \in \tilde{\mathbf{P}}_{\geq m} \mid [P, \mathbf{S}'] \neq 0\}. \tag{48}
\end{aligned}$$

According to the definition in Eq. (46) we now conclude

$$\mathbf{S}' \in \mathcal{S}(\mathbb{T}_{m-2k+2, m-1}(\tilde{\mathbf{P}}_{< m})). \tag{49}$$

Since any $P \in \mathbf{P}_{<m}$ with $\mathbb{T}_{m-2k+2,m-1} \neq I$ must have $q_P^{\text{last}} \geq m - 2k + 2$, $\mathbb{T}_{m-2k+2,m-1}(\tilde{\mathbf{P}}_{<m})$ has at most $(2k-2)M$ non-identity elements. Also \mathbf{S}' is a $2k-2$ qubit stabilizer group. According to Lemma 2, there are at most $(2(2k-2)M)^{2k-1}$ choices of \mathbf{S}' .

Finally, we have

$$\mathbf{S}_{\text{right}}^m \subseteq \mathcal{S}(\mathbb{T}_{m-k+1,m}(\tilde{\mathbf{P}}_{\geq m} - \tilde{\mathbf{P}}_{\text{invalid}}^m)) \subseteq \mathcal{S}(\mathbb{T}_{m-k+1,m}(\tilde{\mathbf{P}}_{\geq m})). \quad (50)$$

For a similar reason, there are at most kM non-identity elements in $\mathbb{T}_{m-k+1,m}(\tilde{\mathbf{P}}_{\geq m})$. Thus there are at most $(2kM)^{k+1}$ choices of $\mathbf{S}_{\text{right}}^m$.

Combining the above two upper bounds, there are at most $(2(2k-2)M)^{2k-1} \cdot (2kM)^{k+1} < (4kM)^{3k}$ different candidates values of A_m . Also both $\mathbb{T}_{m-k+1,m}(\tilde{\mathbf{P}}_{\geq m})$ and $\mathbb{T}_{m-2k+2,m-1}(\tilde{\mathbf{P}}_{<m})$ can be determined by $\mathbb{T}_{m-2k+2,m}(\tilde{\mathbf{P}})$. Thus the candidates of A_m can be determined by $\mathbb{T}_{m-2k+2,m}(\tilde{\mathbf{P}})$. \square

E. Proof of Theorem 3

Proof. We first consider the Hamiltonian on a finite chain with n sites. We denote the Hamiltonian with n sites as H_n . According to the exact 1D local algorithm, we can start from $A_0 = A_0(\emptyset)$ at the beginning and generate $\{A_{m=0}^{n+1}\}$ by $A_{m+1} \in F(A_m)$. Following the proof of Lemma 6, there are at most N_A candidate values of A_m . These candidate values of A_m are fully determined by the surrounding environment $\tilde{\mathbf{P}}_{\text{local}}(m) = \mathbb{T}_{m-2k+2,m}(\tilde{\mathbf{P}})$ which is again periodic, i.e. $\tilde{\mathbf{P}}_{\text{local}}(m) = \tilde{\mathbf{P}}_{\text{local}}(m+l)$. Thus for those $m > 2k-2$ differ by multiples of l , they have the same (and finite) candidate values of A_m . Thus there must exist $A_{m=c_1l} = A_{m=c_2l}$ with $c_2 - c_1 \leq N_A$.

Now we prove that the stabilizer ground state energy per site of the infinite Hamiltonian is

$$\tilde{E}_{\min} = \min_{A_{c_2l} = A_{c_1l}} \frac{E_{\text{gs}}(A_{c_2l}) - E_{\text{gs}}(A_{c_1l})}{(c_2 - c_1)l}, \quad (51)$$

where $E_{\text{gs}}(A_m)$ is defined in Definition 8. If there exists an infinite stabilizer state with a lower per-site energy than \tilde{E}_{\min} , then for sufficiently large n , the stabilizer ground state energy $E_{\min}^{(n)}$ of the finite Hamiltonian $H_n = \sum_{P \in \mathbf{P}} w_P P$ can be lower than $n\tilde{E}_{\min}$ by arbitrary amount of energy E_C , i.e. $E_{\min}^{(n)} \leq n\tilde{E}_{\min} - E_C$. Let the stabilizer group of the corresponding stabilizer state be $\mathbf{S} = \langle \mathbf{Q} \rangle$, $\mathbf{Q} \in \mathcal{S}(\mathbf{P})$, and let $A_m = A_m(\mathbf{Q})$ for each m . If $n > N_A l$, we can find $0 \leq c_1 \leq c_2 \leq n$ such that $A_{c_1l} = A_{c_2l} = A$. Then we have $\Delta E = E_{\text{gs}}(A_{c_2l}) - E_{\text{gs}}(A_{c_1l}) \geq (c_2 - c_1)\tilde{E}_{\min}$ according to the definition of \tilde{E}_{\min} . Now we remove $\{A_{i=c_1+1}^{c_2}\}$ from the path $\{A_{i=0}^{n+1}\}$, and consider the new path $\{A'_i | 0 \leq i \leq n'\} = \{A_0, A_1, \dots, A_{c_1l-1}, A, A_{c_2l+1}, A_{c_2l+2}, \dots, A_n\}$, where $n' = n - (c_2 - c_1)l$. In fact, it still satisfies $A'_{m+1} \in F(A'_m)$ for each m , thus it exactly maps to the stabilizer ground state of $H_{n'}$ with energy $E^{(n')} = E_{\min}^{(n)} - \Delta E \leq E_{\min}^{(n)} - (c_2 - c_1)\tilde{E}_{\min} \leq n'\tilde{E}_{\min} - E_C$. We can then continue the above deleting process and create $\{A''_i | 0 \leq i \leq n''\}$, $\{A'''_i | 0 \leq i \leq n'''\}$, ..., until we end up with some $n^* \leq N_A l$ and the corresponding path $\{A^*_i | 0 \leq i \leq n^*\}$. Such a path can map to some n^* -qubit stabilizer state $|\psi^*\rangle$ with energy $\langle \psi^* | H_{n^*} | \psi^* \rangle = E^{(n^*)} \leq n^*\tilde{E}_{\min} - E_C$. However $\langle \psi^* | H_{n^*} | \psi^* \rangle$ should have a finite lower bound in the order of $O(N_A l)$, which is independent of n . Thus E_C cannot be arbitrarily large, which conflicts with the assumption. Thus we conclude that \tilde{E}_{\min} is the stabilizer ground state energy per site.

Let c_1 , c_2 and $A_{c_1l} = A_{c_2l} = A$ minimize Eq. (51). Let $\{A_{m=c_1}^{c_2}\}$ be one of the path satisfies $A_{m+1} \in F(A_m)$. We can construct a stabilizer state with the stabilizer group $\mathbf{S} = \langle \mathbf{Q} \rangle$ with $\mathbf{Q}_m = \mathbf{S}_{\text{right}}^{m'} \cap \tilde{\mathbf{P}}_{m'}$ for each m , where $c_1 \leq m' < c_2$ satisfies $m' = m \pmod{c}$, where $c = c_2 - c_1$ is the supercell size. According to Corollary 3, this state gives exactly the per-site energy \tilde{E}_{\min} , thus it is (one of) the stabilizer ground state of the infinite periodic Hamiltonian H . The corresponding path $\{A_{m=-\infty}^{\infty}\}$ thus satisfies $A_m = A_{m+cl}$ for any m . \square

[1] A. Kitaev, A. H. Shen, and M. N. Vyalyi, *Classical and Quantum Computation*, 47 (American Mathematical Soc., Providence, 2002).
[2] D. Aharonov and T. Naveh, Quantum NP - A Survey, arXiv:quant-ph/0210077 (2002), [arXiv:quant-ph/0210077](https://arxiv.org/abs/quant-ph/0210077).
[3] J. Kempe, A. Kitaev, and O. Regev, The complexity of the local Hamiltonian problem, *SIAM J. Comput.* **35**, 1070 (2006).
[4] N. Schuch and F. Verstraete, Computational complexity of interacting electrons and fundamental limitations of density functional theory, *Nat. Phys.* **5**, 732 (2009).

[5] Y. Huang, Two-dimensional local Hamiltonian problem with area laws is QMA-complete, *J. Comput. Phys.* **443**, 110534 (2021).

[6] S. Lee, J. Lee, H. Zhai, Y. Tong, A. M. Dalzell, A. Kumar, P. Helms, J. Gray, Z.-H. Cui, W. Liu, *et al.*, Evaluating the evidence for exponential quantum advantage in ground-state quantum chemistry, *Nat. Commun.* **14**, 1952 (2023).

[7] F. Verstraete, V. Murg, and J. Cirac, Matrix product states, projected entangled pair states, and variational renormalization group methods for quantum spin systems, *Adv. Phys.* **57**, 143 (2008).

[8] U. Schollwöck, The density-matrix renormalization group in the age of matrix product states, *Ann. Phys.* **326**, 96 (2011).

[9] H.-J. Liao, J.-G. Liu, L. Wang, and T. Xiang, Differentiable programming tensor networks, *Phys. Rev. X* **9**, 31041 (2019).

[10] G. Carleo and M. Troyer, Solving the quantum many-body problem with artificial neural networks, *Science* **355**, 602 (2017).

[11] D.-L. Deng, X. Li, and S. Das Sarma, Quantum entanglement in neural network states, *Phys. Rev. X* **7**, 021021 (2017).

[12] I. Glasser, N. Pancotti, M. August, I. D. Rodriguez, and J. I. Cirac, Neural-network quantum states, string-bond states, and chiral topological states, *Phys. Rev. X* **8**, 11006 (2018).

[13] J. Chen, S. Cheng, H. Xie, L. Wang, and T. Xiang, Equivalence of restricted Boltzmann machines and tensor network states, *Phys. Rev. B* **97**, 085104 (2018).

[14] S.-X. Zhang, Z.-Q. Wan, and H. Yao, Automatic differentiable Monte Carlo: Theory and application, *Phys. Rev. Res.* **5**, 033041 (2023).

[15] X.-Q. Sun, T. Nebabu, X. Han, M. O. Flynn, and X.-L. Qi, Entanglement features of random neural network quantum states, *Phys. Rev. B* **106**, 115138 (2022).

[16] R. Shankar, *Principles of quantum mechanics* (Springer Science & Business Media, 2012).

[17] C. Møller and M. S. Plesset, Note on an approximation treatment for many-electron systems, *Phys. Rev.* **46**, 618 (1934).

[18] I. Shavitt and R. J. Bartlett, *Many-body methods in chemistry and physics: MBPT and coupled-cluster theory* (Cambridge university press, 2009).

[19] R. J. Bartlett and M. Musiał, Coupled-cluster theory in quantum chemistry, *Rev. Mod. Phys.* **79**, 291 (2007).

[20] I. N. Levine, D. H. Busch, and H. Shull, *Quantum chemistry*, Vol. 6 (Pearson Prentice Hall Upper Saddle River, NJ, 2009).

[21] A. Szabo and N. S. Ostlund, *Modern quantum chemistry: Introduction to advanced electronic structure theory* (Courier Corporation, 2012).

[22] M. A. Nielsen and I. L. Chuang, Quantum computation and quantum information, *Phys. Today* **54**, 60 (2001).

[23] D. Gottesman, Theory of fault-tolerant quantum computation, *Phys. Rev. A* **57**, 127 (1998).

[24] D. Gottesman, The Heisenberg representation of quantum computers, arXiv preprint quant-ph/9807006 (1998).

[25] S. Aaronson and D. Gottesman, Improved simulation of stabilizer circuits, *Phys. Rev. A* **70**, 052328 (2004).

[26] P. Jordan and E. P. Wigner, *Über das paulische äquivalenzverbot* (Springer, 1993).

[27] S. B. Bravyi and A. Y. Kitaev, Fermionic quantum computation, *Ann. Phys.* **298**, 210 (2002).

[28] A. Macridin, P. Spentzouris, J. Amundson, and R. Harnik, Electron-phonon systems on a universal quantum computer, *Phys. Rev. Lett.* **121**, 110504 (2018).

[29] A. Miessen, P. J. Ollitrault, and I. Tavernelli, Quantum algorithms for quantum dynamics: A performance study on the spin-boson model, *Phys. Rev. Res.* **3**, 043212 (2021).

[30] O. Di Matteo, A. McCoy, P. Gysbers, T. Miyagi, R. M. Woloshyn, and P. Navrátil, Improving Hamiltonian encodings with the Gray code, *Phys. Rev. A* **103**, 042405 (2021).

[31] W. Li, J. Ren, S. Huai, T. Cai, Z. Shuai, and S. Zhang, Efficient quantum simulation of electron-phonon systems by variational basis state encoder, *Phys. Rev. Res.* **5**, 023046 (2023).

[32] B. Zeng, X. Chen, D.-L. Zhou, and X.-G. Wen, *Quantum Information Meets Quantum Matter*, Quantum Science and Technology (Springer New York, New York, NY, 2019).

[33] D. Perez-Garcia, F. Verstraete, M. M. Wolf, and J. I. Cirac, Matrix product state representations, arXiv preprint quant-ph/0608197 (2006).

[34] D. Fattal, T. S. Cubitt, Y. Yamamoto, S. Bravyi, and I. L. Chuang, Entanglement in the stabilizer formalism, arXiv preprint quant-ph/0406168 (2004).

[35] Z. Webb, The Clifford group forms a unitary 3-design, *Quantum Info. Comput.* **16**, 1379–1400 (2016).

[36] H. Y. Huang, R. Kueng, and J. Preskill, Predicting many properties of a quantum system from very few measurements, *Nat. Phys.* **16**, 1050 (2020).

[37] A. Nahum, J. Ruhman, S. Vijay, and J. Haah, Quantum entanglement growth under random unitary dynamics, *Phys. Rev. X* **7**, 031016 (2017).

[38] C. W. von Keyserlingk, T. Rakovszky, F. Pollmann, and S. L. Sondhi, Operator hydrodynamics, OTOCs, and entanglement growth in systems without conservation laws, *Phys. Rev. X* **8**, 021013 (2018).

[39] A. Nahum, S. Vijay, and J. Haah, Operator spreading in random unitary circuits, *Phys. Rev. X* **8**, 021014 (2018).

[40] D. Gottesman, Stabilizer codes and quantum error correction, arXiv preprint quant-ph/9705052 (1997).

[41] A. G. Fowler, M. Mariantoni, J. M. Martinis, and A. N. Cleland, Surface codes: Towards practical large-scale quantum computation, *Phys. Rev. A* **86**, 032324 (2012).

[42] C. Nayak, S. H. Simon, A. Stern, M. Freedman, and S. Das Sarma, Non-Abelian anyons and topological quantum computation, *Rev. Mod. Phys.* **80**, 1083 (2008).

[43] S. Bravyi, D. Browne, P. Calpin, E. Campbell, D. Gosset, and M. Howard, Simulation of quantum circuits by low-rank stabilizer decompositions, *Quantum* **3**, 181 (2019).

[44] S. Bravyi and D. Gosset, Improved classical simulation of quantum circuits dominated by Clifford gates, *Phys. Rev. Lett.*

116, 250501 (2016).

[45] T. Begušić, K. Hejazi, and G. K. Chan, Simulating quantum circuit expectation values by clifford perturbation theory, arXiv preprint arXiv:2306.04797 (2023).

[46] M. Cheng, K. Khosla, C. Self, M. Lin, B. Li, A. Medina, and M. Kim, Clifford circuit initialisation for variational quantum algorithms, arXiv preprint arXiv:2207.01539 (2022).

[47] S. Zhang, Z.-Q. Wan, C.-Y. Hsieh, H. Yao, and S. Zhang, Variational quantum-neural hybrid error mitigation, *Adv. Quantum Technol.* **6** (2023).

[48] J. Sun, L. Cheng, and W. Li, Toward chemical accuracy with shallow quantum circuits: A Clifford-based Hamiltonian engineering approach, *J. Chem. Theory Comput.* **20**, 695 (2024).

[49] R. V. Mishmash, T. P. Gujarati, M. Motta, H. Zhai, G. K.-L. Chan, and A. Mezzacapo, Hierarchical Clifford transformations to reduce entanglement in quantum chemistry wave functions, *J. Chem. Theory Comput.* (2023).

[50] P. Schleich, J. Boen, L. Cincio, A. Anand, J. S. Kottmann, S. Tretiak, P. A. Dub, and A. Aspuru-Guzik, Partitioning quantum chemistry simulations with clifford circuits, arXiv preprint arXiv:2303.01221 (2023).

[51] D. Gross, Hudson's theorem for finite-dimensional quantum systems, *J. Math. Phys.* **47** (2006).

[52] J. E. Hopcroft, R. Motwani, and J. D. Ullman, Introduction to automata theory, languages, and computation, Acm Sigact News **32**, 60 (2001).

[53] A. Salomaa, *Theory of automata* (Elsevier, 2014).

[54] F. Bloch, Über die quantenmechanik der elektronen in kristallgittern, *Zeitschrift für physik* **52**, 555 (1929).

[55] P. Kratzer and J. Neugebauer, The basics of electronic structure theory for periodic systems, *Front. Chem.* **7**, 106 (2019).

[56] R. M. Martin, *Electronic structure: basic theory and practical methods* (Cambridge university press, 2020).

[57] A. Y. Kitaev, Fault-tolerant quantum computation by anyons, *Ann. Phys.* **303**, 2 (2003).

[58] G. S. Ravi, P. Gokhale, Y. Ding, W. Kirby, K. Smith, J. M. Baker, P. J. Love, H. Hoffmann, K. R. Brown, and F. T. Chong, Cafqa: A classical simulation bootstrap for variational quantum algorithms, in *Proceedings of the 28th ACM International Conference on Architectural Support for Programming Languages and Operating Systems, Volume 1* (2022) pp. 15–29.

[59] R. Koenig and J. A. Smolin, How to efficiently select an arbitrary Clifford group element, *J. Math. Phys.* **55** (2014).

[60] B. Bhattacharyya and G. S. Ravi, Optimal Clifford initial states for Ising Hamiltonians, in *2023 IEEE International Conference on Rebooting Computing (ICRC)* (IEEE, 2023) pp. 1–10.

[61] M. Cerezo, A. Sone, T. Volkoff, L. Cincio, and P. J. Coles, Cost function dependent barren plateaus in shallow parametrized quantum circuits, *Nat. Commun.* **12**, 1791 (2021).

[62] J. R. McClean, S. Boixo, V. N. Smelyanskiy, R. Babbush, and H. Neven, Barren plateaus in quantum neural network training landscapes, *Nat. Commun.* **9**, 4812 (2018).

[63] H.-K. Zhang, S. Liu, and S.-X. Zhang, Absence of barren plateaus in finite local-depth circuits with long-range entanglement, arXiv:2311.01393 (2023).

[64] Z.-X. Shang, M.-C. Chen, X. Yuan, C.-Y. Lu, and J.-W. Pan, Schrödinger-Heisenberg variational quantum algorithms, *Phys. Rev. Lett.* **131**, 060406 (2023).

[65] Y. Kim, A. Eddins, S. Anand, K. X. Wei, E. Van Den Berg, S. Rosenblatt, H. Nayfeh, Y. Wu, M. Zaletel, K. Temme, *et al.*, Evidence for the utility of quantum computing before fault tolerance, *Nature* **618**, 500 (2023).

[66] F. Arute, K. Arya, R. Babbush, D. Bacon, J. C. Bardin, R. Barends, R. Biswas, S. Boixo, F. G. Brandao, D. A. Buell, *et al.*, Quantum supremacy using a programmable superconducting processor, *Nature* **574**, 505 (2019).

[67] R. Wiersema, C. Zhou, Y. de Sereville, J. F. Carrasquilla, Y. B. Kim, and H. Yuen, Exploring entanglement and optimization within the Hamiltonian variational ansatz, *PRX Quantum* **1**, 020319 (2020).

[68] S.-X. Zhang, J. Allcock, Z.-Q. Wan, S. Liu, J. Sun, H. Yu, X.-H. Yang, J. Qiu, Z. Ye, Y.-Q. Chen, C.-K. Lee, Y.-C. Zheng, S.-K. Jian, H. Yao, C.-Y. Hsieh, and S. Zhang, Tensorcircuit: A quantum software framework for the NISQ era, *Quantum* **7**, 912 (2023).

[69] R. H. Byrd, P. Lu, J. Nocedal, and C. Zhu, A limited memory algorithm for bound constrained optimization, *SIAM J. Sci. Comput.* **16**, 1190 (1995).

[70] P. Virtanen, R. Gommers, T. E. Oliphant, M. Haberland, T. Reddy, D. Cournapeau, E. Burovski, P. Peterson, W. Weckesser, J. Bright, S. J. van der Walt, M. Brett, J. Wilson, K. J. Millman, N. Mayorov, A. R. J. Nelson, E. Jones, R. Kern, E. Larson, C. J. Carey, İ. Polat, Y. Feng, E. W. Moore, J. VanderPlas, D. Laxalde, J. Perktold, R. Cimrman, I. Henriksen, E. A. Quintero, C. R. Harris, A. M. Archibald, A. H. Ribeiro, F. Pedregosa, P. van Mulbregt, and SciPy 1.0 Contributors, SciPy 1.0: Fundamental algorithms for scientific computing in Python, *Nat. Methods* **17**, 261 (2020).

[71] R. Verresen, R. Moessner, and F. Pollmann, One-dimensional symmetry protected topological phases and their transitions, *Phys. Rev. B* **96**, 165124 (2017).

[72] F. Wu, Y. Deng, and N. Prokof'ev, Phase diagram of the toric code model in a parallel magnetic field, *Phys. Rev. B* **85**, 195104 (2012).

[73] F. Barahona, On the computational complexity of Ising spin glass models, *J. Phys. A Math. Gen.* **15**, 3241 (1982).

[74] S.-X. Zhang, Classification on the computational complexity of spin models, arXiv preprint arXiv:1911.04122 (2019).

[75] S.-X. Zhang, C.-Y. Hsieh, S. Zhang, and H. Yao, Differentiable quantum architecture search, *Quantum Sci. Technol.* **7**, 045023 (2022).

[76] A. Gu, H.-Y. Hu, D. Luo, T. L. Patti, N. C. Rubin, and S. F. Yelin, Zero and finite temperature quantum simulations powered by quantum magic, arXiv preprint arXiv:2308.11616 (2023).